Well posedness of fully coupled fracture/bulk Darcy Flow with XFEM

Marco Del Pra† Alessio Fumagalli♯ Anna Scotti♯

May 19, 2015

†*Past affiliation:* Department of Mathematics "Federigo Enriques"
Università degli Studi di Milano
via Cesare Saldini 50, 20133 Milan, Italy
`marcodelpra@hotmail.it`

♯ MOX– Modellistica e Calcolo Scientifico
Dipartimento di Matematica "F. Brioschi"
Politecnico di Milano
via Bonardi 9, 20133 Milano, Italy
`alessio.fumagalli@mail.polimi.it`
`anna.scotti@mail.polimi.it`

Keywords: Flows in fractured porous media, stability of mixed finite element, extended finite element

Abstract

In this work we consider the coupled problem of Darcy's flow in a fracture and the surrounding porous medium. The fracture is represented as a $(d-1)$-dimensional interface and it is non-matching with the computational grid thanks to a suitable XFEM enrichment of the mixed finite element spaces. In the existing literature well posedness has been proven for the discrete problem in the hypothesis of given solution in the fracture. This works provides theoretical results on the stability and convergence of the discrete, fully coupled problem, yielding sharp conditions on the fracture geometry and on the computational grid to ensure that the inf-sup conditions is satisfied by the enriched spaces, as confirmed by numerical experiments.

1 Introduction

The simulation of flow in fractured porous media has become, in the last decade, a fundamental tool for many energy-related engineering applications such as the exploitation of oil reservoirs and geothermal fields, or the safe long term storage of CO_2 and nuclear waste. In all the aforementioned applications an accurate and reliable numerical simulation can support decision making and risk assessment. One of the main difficulties for this type of problems is the intrinsic inhomogeneity of the porous medium, particularly in the presence of fractures. Traditional approaches to account for the presence of fractures consist in modifications of the permeability tensor, or in semi-empirical transfer functions to be applied in the dual-porosity framework [8]. These approaches, however, are not sufficient in the case of disconnected, non-homogeneous and anisotropic fracture distributions. For this reason the direct simulation of fractures immersed in a porous matrix has become more and more popular. Very often fractures are represented as $(d-1)$-dimensional interfaces immersed in a d-dimensional matrix, due to their spatial scale. Indeed, their typical width is, at all scales, very small compared to the length and to the typical size of the domain of interest and the use of a geometrically reduced model avoids the need for extremely refined or anisotropic grids inside the fractures. In this work we adopt a reduced model for flow in fractures based on the work by Alboin et al., [2] for single-phase flow, together with suitable coupling conditions between fracture and bulk flow. The formulation, originally derived in [2] only for permeable fractures, was then extended in [20] and [3] to more general coupling conditions (for low-permeability fractures) and geometric configurations (for "immersed" fractures, *i.e.* fractures that do not cut the entire domain). We also point out that this approach can be extended to two-phase flow as shown in [18]. All the aforementioned works rely on the hypothesis of conformal or quasi-conformal grids, *i.e.* the edges of the grids must be aligned with the fractures. In realistic cases geometric conformity can represent a constraint that may possibly affect the quality of the resulting grid, even in two-dimensional cases if the number of fractures is large, or if we have intersections with small angles, or nearly coincident fractures. For most numerical methods a poor quality of the grid reflects on the accuracy of the solution. Different approaches have been proposed to tackle this difficulty. On one hand, one could take advantage of the fact that the actual position of the fractures is always affected by uncertainty, and modify the fracture network to avoid such problems [19]. Another possibility is to use methods that are robust even in the presence of highly distorted grids, such as Mimetic Finite Differences and the Virtual Element Method, [5, 1, 4]. Finally, the approach adopted in this work consists in avoiding geometric conformity in the first place, using eXtended Finite Elements (XFEM): thanks to suitable enrichments of the FEM spaces we allow fractures to cut the elements of the grid. In particular, we employ the method originally proposed in [7], which is based on the enrichment technique described in [17]. Even if the method has been successfully used in simple configurations and extended to the two-phase case [12] and networks [11, 14] some theoretical aspects still needed to be investigated. In particular, in this paper we provide a proof of the well-posedness of the discrete, fully coupled, matrix-fracture problem. Indeed, in [7] the well-posedness is proven with in the assumption that the solution in the fracture is given. We point out that, since we are using non-matching grids, the inf-sup condition for the coupled problem is only conditionally satisfied even if the unbroken FEM spaces are individually inf-sup stable. We also prove by numerical experiments that the method exhibits the theoretical convergence rate.

The paper is organized as follows. In Section 2 we briefly recall the mathematical model for single-phase Darcy flow in the fracture-matrix system. In Section 3 we describe the numerical discretization by means of the XFEM. Section 4 is dedicated to the proof of the well posedness of the discrete problem. In Section 5 we present some numerical experiments, and finally, in Section 6 we discuss conclusions and further developments.

2 The mathematical model

In this section we present the mathematical framework for Darcy's flow in fractured porous media. In Subsection 2.1 we consider the standard physical problem of a single-phase flowing in a porous medium. Then, in Subsection 2.2 we introduce the reduced model on the $(d-1)$-domain to handle in an effective way the fracture flow problem.

2.1 Physical problem

We consider a computational domain Ω, representation of the physical porous medium, connected and open subset of $\mathbb{R}^d$. The boundary of Ω, supposed regular enough, is indicated by $\Gamma := \partial\Omega$ and divided in Dirichlet and Neumann disjoint parts: Γ_D and Γ_N, respectively, such that $\overline{\Gamma} = \overline{\Gamma_D} \cup \overline{\Gamma_N}$. We assume that Ω contains a proper subset Ω_f representing the fracture such that $\Omega \setminus \overline{\Omega_f}$ is made of two disjoint, connected and open subset of Ω. These set are indicated by Ω_i and represent the surrounding porous media of the fracture. Throughout this work we indicate with a subscript (normally i, j or f) the restriction of unknown functions and data to the corresponding part of Ω. Following [20, 7] we suppose that the fracture can be written as

$$\Omega_f = \left\{ \boldsymbol{x} \in \mathbb{R}^d : \boldsymbol{x} = \boldsymbol{s} + r\boldsymbol{n}_{\hat{\gamma}}, \boldsymbol{s} \in \hat{\gamma}, |r| < l_{\hat{\gamma}}/2 \right\},$$

where $l_{\hat{\gamma}} > 0$ is the thickness of the fracture in the normal direction, which can be function of $\boldsymbol{s}$, $\hat{\gamma} \subset \mathbb{R}^{d-1}$ is the non-intersecting one co-dimensional centre of the fracture and $\boldsymbol{n}_{\hat{\gamma}}$ is the continuous unit normal vector field on $\hat{\gamma}$ pointing outward from Ω_1 toward Ω_2. We suppose that the thickness $l_{\hat{\gamma}}$ is much smaller than the other sizes of the fracture, the typical dimension of the domain Ω and the grid size introduced in the forthcoming section. We indicate by $\hat{\gamma}_i$ the boundary of Ω_f in contact with Ω_i and by $\boldsymbol{n}_{\hat{\gamma}_j}$ the continuous unit normal field on $\hat{\gamma}_i$ pointing outward from Ω_f toward Ω_i. See Figure 1a for an example of fractured domain. Our objective is to compute the pressure field p and the Darcy velocity field $\boldsymbol{u}$

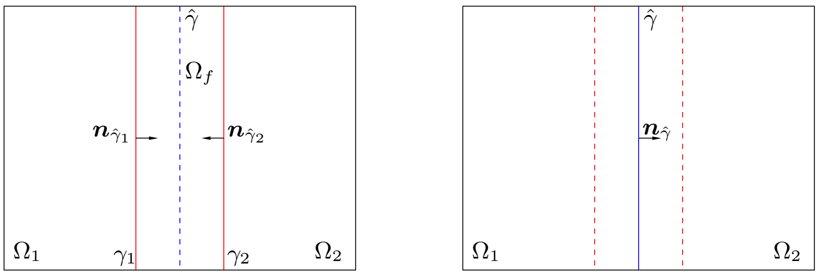

(a) Original domain. (b) Reduced domain.

Figure 1: Representation of each sub-domain.

solution of the transmission problem for $i = 1, 2, f$ and $j = 1, 2$

$$\begin{cases} \nabla \cdot \boldsymbol{u}_i = f_i \\ \boldsymbol{u}_i = -\boldsymbol{\Lambda}_i \left(\nabla p_i - \boldsymbol{f}_i \right) \end{cases} \text{in } \Omega_i \qquad \begin{cases} p_j = p_f \\ \boldsymbol{u}_j \cdot \boldsymbol{n}_{\hat{\gamma}_j} = \boldsymbol{u}_f \cdot \boldsymbol{n}_{\hat{\gamma}_j} \end{cases} \text{on } \hat{\gamma}_j \tag{1a}$$

with boundary conditions

$$\begin{cases} p_i = p_{0i} & \text{on } \Gamma_{Ni} \\ \boldsymbol{u}_i \cdot \boldsymbol{n}_\Gamma = u_{0i} & \text{on } \Gamma_{Di} \end{cases}, \tag{1b}$$

where $\boldsymbol{\Lambda}_i \in [L^\infty(\Omega_i)]^{d \times d}$ is the elliptic permeability tensor, $f_i \in L^2(\Omega_i)$ a scalar source/sink term, $\boldsymbol{f}_i \in [L^2(\Omega_i)]^d$ a vector forcing term, $p_{i0} \in H^{\frac{1}{2}}(\Gamma_{Ni})$ the Neumann boundary data and $u_{i0} \in L^2(\Gamma_{Ni})$ the Dirichlet boundary data. The weak formulation of problem (1) is well posed, see for example [6, 21, 9, 22].

2.2 Reduced model

To ease the presentation we consider bidimensional domains $d = 2$. Following [10, 20, 7, 13] we employ a model reduction strategy to introduce a new set of equations which can handle the fracture as object of codimension one. In this procedure we will substitute the fracture Ω_f by its centre axis $\hat{\gamma}$ with boundary $\partial\hat{\gamma}$. We suppose that the latter is divided into a Dirichlet part $\partial_D\hat{\gamma}$, approximation of Γ_{Df}, and a Neumann part $\partial_N\hat{\gamma}$, approximation of Γ_{Nf}. We indicate by $\boldsymbol{\tau}_{\hat{\gamma}}$ the continuous unit normal tangential vector of the fracture $\hat{\gamma}$. See Figure 1b for an example. We suppose that the permeability can be written as $\boldsymbol{\Lambda}_f = \lambda_{f,\boldsymbol{n}}\boldsymbol{N} + \lambda_{f,\boldsymbol{\tau}}\boldsymbol{T}$ in the fracture and $\boldsymbol{\Lambda}_i = \eta_i^{-1}\boldsymbol{I}$ in each i-th part of the surrounding porous media, where $\boldsymbol{N} := \boldsymbol{n}_{\hat{\gamma}} \otimes \boldsymbol{n}_{\hat{\gamma}}$ and $\boldsymbol{T} := \boldsymbol{I} - \boldsymbol{N}$ are the projection matrices on the normal and tangential space of the fracture $\hat{\gamma}$, respectively. We will make use of the normal and tangential divergence and gradient operators $\nabla_{\boldsymbol{n}}\cdot := \boldsymbol{N} : \nabla$, $\nabla_{\boldsymbol{\tau}}\cdot := \boldsymbol{T} : \nabla$, $\nabla_{\boldsymbol{n}} := \boldsymbol{N}\nabla$ and $\nabla_{\boldsymbol{\tau}} := \boldsymbol{T}\nabla$. We indicate by $(\cdot,\cdot)_A$ the scalar product in $L^2(A)$. The data and unknowns defined on $\hat{\gamma}$ are called "reduced" and indicated with the hat notation $\hat{\cdot}$. We introduce the reduced pressure $\hat{p}$, reduced Darcy velocity $\hat{\boldsymbol{u}}$ and the inverse of the effective normal and tangential reduced permeability as

$$\hat{p}(\boldsymbol{s}) := \frac{1}{l_{\hat{\gamma}}}\left(p,1\right)_{\omega} \quad \hat{\boldsymbol{u}}(\boldsymbol{s}) := \left(\boldsymbol{T}\boldsymbol{u}_f, 1\right)_{\omega} \quad \hat{\eta}(\boldsymbol{s}) := \frac{1}{l_{\hat{\gamma}}\lambda_{f,\boldsymbol{\tau}}} \quad \eta_{\hat{\gamma}}(\boldsymbol{s}) := \frac{l_{\hat{\gamma}}}{\lambda_{f,\boldsymbol{n}}},$$

with $\boldsymbol{s} \in \hat{\gamma}$ and $\omega(\boldsymbol{s}) = \left(-\frac{l_{\hat{\gamma}}(\boldsymbol{s})}{2}, \frac{l_{\hat{\gamma}}(\boldsymbol{s})}{2}\right)$, the vector and scalar data of (1) are reduced in the same way as $\hat{\boldsymbol{u}}$ and $\hat{p}$, respectively. The system of equations for single phase flow in the two subdomains $\Omega_j,\ j = 1, 2$, and on the reduced domain $\hat{\gamma}$ is the following

$$\begin{cases} \nabla\cdot\boldsymbol{u}_j = f_j & \text{in } \Omega_j \\ \eta_j\boldsymbol{u}_j + \nabla p_j = \boldsymbol{f}_j & \\ p_j = p_0 & \text{on } \Gamma_{Nj} \\ \boldsymbol{u}_j\cdot\boldsymbol{n} = u_{0j} & \text{on } \Gamma_{Dj} \end{cases} \qquad \begin{cases} \nabla_{\boldsymbol{\tau}}\cdot\hat{\boldsymbol{u}} = l_{\hat{\gamma}}\hat{f} + [\![\boldsymbol{u}\cdot\boldsymbol{n}_{\hat{\gamma}}]\!] & \text{in } \hat{\gamma} \\ \hat{\eta}\hat{\boldsymbol{u}} + \nabla_{\boldsymbol{\tau}}\hat{p} = \hat{\boldsymbol{f}} & \\ \hat{p} = \hat{p}_0 & \text{on } \partial_N\hat{\gamma} \\ \hat{\boldsymbol{u}}\cdot\boldsymbol{\tau}_{\hat{\gamma}} = \hat{u}_0 & \text{on } \partial_D\hat{\gamma} \end{cases} \tag{2a}$$

with the coupling conditions [20]

$$\begin{cases} \eta_{\hat{\gamma}}\,\{\!\{\boldsymbol{u}\cdot\boldsymbol{n}_{\hat{\gamma}}\}\!\} = [\![p]\!] + l_{\hat{\gamma}}\,\{\!\{\boldsymbol{f}\cdot\boldsymbol{n}_{\hat{\gamma}}\}\!\} \\ \xi_0\eta_{\hat{\gamma}}[\![\boldsymbol{u}\cdot\boldsymbol{n}_{\hat{\gamma}}]\!] + \dfrac{l_{\hat{\gamma}}}{4}[\![\boldsymbol{f}\cdot\boldsymbol{n}_{\hat{\gamma}}]\!] = \{\!\{p\}\!\} - \hat{p} \end{cases} \quad \text{on } \hat{\gamma}. \tag{2b}$$

In the previous system we have indicated with $[\![a]\!] := a_1|_{\hat{\gamma}} - a_2|_{\hat{\gamma}}$ the jump operator and with $\{\!\{a\}\!\} := \frac{1}{2}(a_1|_{\hat{\gamma}} + a_2|_{\hat{\gamma}})$ the mean operator across $\hat{\gamma}$. With an abuse of notation for the vector field we have $[\![\boldsymbol{a}\cdot\boldsymbol{n}_{\hat{\gamma}}]\!] := \boldsymbol{a}_1\cdot\boldsymbol{n}_{\hat{\gamma}}|_{\hat{\gamma}} - \boldsymbol{a}_2\cdot\boldsymbol{n}_{\hat{\gamma}}|_{\hat{\gamma}}$ and $\{\!\{\boldsymbol{a}\cdot\boldsymbol{n}_{\hat{\gamma}}\}\!\} := \frac{1}{2}(\boldsymbol{a}_1\cdot\boldsymbol{n}_{\hat{\gamma}}|_{\hat{\gamma}} + \boldsymbol{a}_2\cdot\boldsymbol{n}_{\hat{\gamma}}|_{\hat{\gamma}})$. Finally ξ_0 is a model closure parameter, see the aforementioned references for a detailed description.

3 Numerical discretization

Let assume that Ω is a convex polygon, and consider a family of triangulations $\mathcal{T}_h$, *i.e.* collections of triangles, being h the maximal diameter of the elements of $\mathcal{T}_h$. We also introduce a family of triangulations $\hat{\mathcal{T}}_h$ of $\hat{\gamma}$, *i.e.* collections of lines, being $\hat{h}$ the maximal length of the elements of $\hat{\mathcal{T}}_h$. We consider the situation where the two triangulations are irrespective of each other, *i.e.* $\hat{\mathcal{T}}_h$ can cut the elements of $\mathcal{T}_h$. The idea is to enrich the elements cut by an embedded interface with discontinuous functions using XFEM: the finite element spaces for velocity and pressure are constructed replicating the degrees of freedom in the cut elements and restricting the corresponding basis functions to each of the subdomains Ω_i [17]. This method was originally developed for the computational analysis of the evolution of cracks in solid mechanics. Here, as in [7] we follow a similar approach considering Raviart-Thomas finite elements and for the coupled fracture/bulk problems.

Hypothesis 1 *Following [17], we require that the forthcoming hypotheses are satisfied:*

H1. the triangulation $\mathcal{T}_h$ is shape-regular, i.e. $\rho_K \lesssim h_K \lesssim \rho_K$ $\forall K \in \mathcal{T}_h$, with h_K the diameter of K and ρ_K the diameter of the largest ball contained in K;

H2. if $\hat{\gamma} \cap K \neq \emptyset$, $K \in \mathcal{T}_h$, then $\hat{\gamma}$ intersects ∂K exactly twice, and each (open) edge at most once.

Where the notation $a \lesssim b$ means that there is a constant $C > 0$, independent of h and of the physical parameters η, $\hat{\eta}$, $\eta_{\hat{\gamma}}$, such that $a \leq Cb$; we will use $a \gtrsim b$ similarly. We define $K_i = K \cap \Omega_i$ for any element $K \in \mathcal{T}_h$, and $\mathcal{G}_h := \{K \in \mathcal{T}_h : \hat{\gamma} \cap K \neq \emptyset\}$ the collection of elements that are cut by the fracture. For any $K \in \mathcal{T}_h$, let $\mathbb{RT}_0(K_i) := \{\boldsymbol{v}_{h|_{K_i}} : \boldsymbol{v}_h \in \mathbb{RT}_0(K)\}$ be the linear space of the restrictions to K_i of the standard $\mathbb{RT}_0$ local functions. We define analogously $\mathbb{P}_0(K_i)$ as the set of functions that are constant on each K_i. Similarly, for any $\hat{K} \in \hat{\mathcal{T}}_h$, we consider $\mathbb{RT}_0(\hat{K})$ and $\mathbb{P}_0(\hat{K})$. We consider discrete velocities $\boldsymbol{v}_h$ and pressures q_h in the following spaces,

$$\mathbf{V}_h := \mathbf{V}_{1,h} \times \mathbf{V}_{2,h} \times \hat{\mathbf{V}}_h, \quad Q_h := Q_{1,h} \times Q_{2,h} \times \hat{Q}_h, \quad \mathbf{W}_h := \mathbf{V}_h \times Q_h$$

where we have defined

$$\begin{aligned}
\mathbf{V}_{i,h} &:= \{\boldsymbol{v}_h \in \boldsymbol{H}_{\mathrm{div}}(\Omega_i) : \ \boldsymbol{v}_{h|_{K_i}} \in \mathbb{RT}_0(K_i) \ \forall K \in \mathcal{T}_h\}, \\
\hat{\mathbf{V}}_h &:= \{\hat{\boldsymbol{v}}_h \in \boldsymbol{H}_{\mathrm{div}}(\hat{\gamma}) : \ \hat{\boldsymbol{v}}_{h|_{\hat{K}}} \in \mathbb{RT}_0(\hat{K}) \ \forall \hat{K} \in \hat{\mathcal{T}}_h\}, \\
Q_{i,h} &:= \{q_h \in L^2(\Omega_i) : \ q_{h|_{K_i}} \in \mathbb{P}_0(K_i) \ \forall K \in \mathcal{T}_h\}, \\
\hat{Q}_h &:= \{\hat{q}_h \in L^2(\hat{\gamma}) : \ \hat{q}_{h|_{\hat{K}}} \in \mathbb{P}_0(\hat{K}) \ \forall \hat{K} \in \hat{\mathcal{T}}_h\}.
\end{aligned}$$

The discrete vector $(\boldsymbol{v}_h, \hat{\boldsymbol{v}}_h) = (\boldsymbol{v}_{1,h}, \boldsymbol{v}_{2,h}, \hat{\boldsymbol{v}}_h)$ and scalar $(q_h, \hat{q}_h) = (q_{1,h}, q_{2,h}, \hat{q}_h)$ fields are thus made of three components, associated to the domains Ω_i, $i = 1, 2$ and to $\hat{\gamma}$. The discrete variables are discontinuous on $\hat{\gamma}$, being defined on each part K_i of a cut element $K \in \mathcal{G}_h$ by independent $(\mathbb{RT}_0, \mathbb{P}_0)$ local functions. The finite element basis for the spaces $\mathbf{V}_{i,h}$ and $Q_{i,h}$ are obtained, following the approach proposed in [17], from the standard $\mathbb{RT}_0$ and $\mathbb{P}_0$ basis on the mesh replacing each standard basis function living on an element that intersects the interface by its restrictions to Ω_i. The numerical scheme can be easily modified to account for variable, tensor valued coefficients. Let us introduce the following

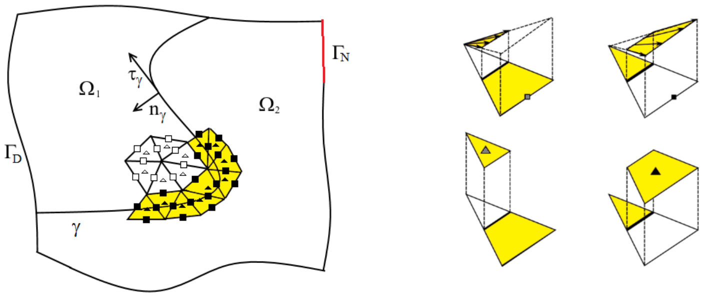

Figure 2: The left part represents the domain Ω and the fracture $\hat{\gamma}$. The boundary $\partial\Omega = \Gamma_D \cup \Gamma_N$ is split in a Dirichlet boundary and a Neumann boundary. Standard $\mathbb{P}_0$ degrees of freedom of the pressure associated to internal nodes (marked with white triangles) are duplicated (black triangles) on elements $K \in \mathcal{G}_h$ crossed by $\hat{\gamma}$ (shaded), to provide constant pressure on each sub-element K_1, K_2. Analogously, the $\mathbb{RT}_0$ degrees of freedom of the velocity, associated to the edges midpoints (white squares) are duplicated (black squares) on elements $K \in \mathcal{G}_h$, leading to independent $\mathbb{RT}_0$ functions on K_1 and K_2, as outlined in the right part.

bilinear and linear forms:

$$\begin{aligned}a(\boldsymbol{u}_h, \hat{\boldsymbol{u}}_h, \boldsymbol{v}_h, \hat{\boldsymbol{v}}_h) :=& (\eta \boldsymbol{u}_h, \boldsymbol{v}_h)_\Omega + \xi_0 \left(\eta_{\hat{\gamma}} [\![\boldsymbol{u}_h \cdot \boldsymbol{n}_{\hat{\gamma}}]\!], [\![\boldsymbol{v}_h \cdot \boldsymbol{n}_{\hat{\gamma}}]\!]\right)_{\hat{\gamma}} \\ &+ \left(\eta_{\hat{\gamma}} \{\!\{\boldsymbol{u}_h \cdot \boldsymbol{n}_{\hat{\gamma}}\}\!\}, \{\!\{\boldsymbol{v}_h \cdot \boldsymbol{n}_{\hat{\gamma}}\}\!\}\right)_{\hat{\gamma}} + \left(\nu h^{-1} \boldsymbol{u}_h \cdot \boldsymbol{n}, \boldsymbol{v}_h \cdot \boldsymbol{n}\right)_{\Gamma_D} \\ &+ (\hat{\eta} \hat{\boldsymbol{u}}_h, \hat{\boldsymbol{v}}_h)_{\hat{\gamma}} + \left(\hat{\nu} \hat{h}^{-1} \hat{\boldsymbol{u}}_h \cdot \boldsymbol{\tau}_{\hat{\gamma}}, \hat{\boldsymbol{v}}_h \cdot \boldsymbol{\tau}_{\hat{\gamma}}\right)_{\partial_D \hat{\gamma}},\end{aligned} \tag{3}$$

$$\begin{aligned}b(p_h, \hat{p}_h, \boldsymbol{v}_h, \hat{\boldsymbol{v}}_h) :=& -(p_h, \nabla \cdot \boldsymbol{v}_h)_\Omega + (p_h, \boldsymbol{v}_h \cdot \boldsymbol{n})_{\Gamma_D} + (\hat{p}_h, [\![\boldsymbol{v}_h \cdot \boldsymbol{n}_{\hat{\gamma}}]\!])_{\hat{\gamma}} \\ &- (\hat{p}_h, \nabla_{\boldsymbol{\tau}} \cdot \hat{\boldsymbol{v}}_h)_{\hat{\gamma}} + (\hat{p}_h, \hat{\boldsymbol{v}}_h \cdot \boldsymbol{\tau}_{\hat{\gamma}})_{\partial_D \hat{\gamma}},\end{aligned} \tag{4}$$

$$\begin{aligned}\mathcal{F}(\boldsymbol{v}_h, \hat{\boldsymbol{v}}_h, q_h, \hat{q}_h) :=& (\boldsymbol{f}, \boldsymbol{v}_h)_\Omega - (p_0, \boldsymbol{v}_h \cdot \boldsymbol{n})_{\Gamma_N} + \left(\nu h^{-1} u_0, \boldsymbol{v}_h \cdot \boldsymbol{n}\right)_{\Gamma_D} \\ &+ (f, q_h)_\Omega - (u_0, q_h)_{\Gamma_D} + \left(\hat{\boldsymbol{f}}, \hat{\boldsymbol{v}}_h\right)_{\hat{\gamma}} - (\hat{p}_0, \hat{\boldsymbol{v}}_h \cdot \boldsymbol{\tau}_{\hat{\gamma}})_{\partial_N \hat{\gamma}} \\ &+ \left(\hat{\nu} \hat{h}^{-1} \hat{u}_0, \hat{\boldsymbol{v}}_h \cdot \boldsymbol{\tau}_{\hat{\gamma}}\right)_{\partial_D \hat{\gamma}} + \left(l_{\hat{\gamma}} \tilde{f}, \hat{q}_h\right)_{\hat{\gamma}} - (\hat{q}_h, \hat{u}_0)_{\partial_D \hat{\gamma}} \\ &+ \left(l_{\hat{\gamma}} \{\!\{\boldsymbol{f} \cdot \boldsymbol{n}_{\hat{\gamma}}\}\!\}, \{\!\{\boldsymbol{v}_h \cdot \boldsymbol{n}_{\hat{\gamma}}\}\!\}\right)_{\hat{\gamma}} - \left(\frac{l_{\hat{\gamma}}}{4} [\![\boldsymbol{f} \cdot \boldsymbol{n}_{\hat{\gamma}}]\!], [\![\boldsymbol{v}_h \cdot \boldsymbol{n}_{\hat{\gamma}}]\!]\right)_{\hat{\gamma}}.\end{aligned} \tag{5}$$

where ν and $\hat{\nu}$ are a positive penalization coefficient that we use to impose Dirichlet boundary conditions and where we denote (with a little abuse of notation) with h and $\hat{h}$ two piecewise constant functions defined respectively on all edges $E \subset \partial K$, $K \in \mathcal{T}_h$ and on all edges $\hat{E} \subset \partial \hat{K}$, $\hat{K} \in \hat{\mathcal{T}}_h$, and such that $h_{|E} := \operatorname{diam}(E)$, $\hat{h}_{|\hat{E}} := \operatorname{diam}(\hat{E})$. Note that in order to ensure the strict positivity of the associated interface term, the assumption $\xi_0 > 0$ is indeed required

[20, 7]. Our finite element method reads as follows: given the boundary data u_0, $\hat{u}_0$, p_0, $\hat{p}_0$, find $(\boldsymbol{u}_h, \hat{\boldsymbol{u}}_h, p_h, \hat{p}_h) \in \mathbf{W}_h$ such that

$$\mathcal{C}\left((\boldsymbol{u}_h, \hat{\boldsymbol{u}}_h, p_h, \hat{p}_h), (\boldsymbol{v}_h, \hat{\boldsymbol{v}}_h, q_h, \hat{q}_h)\right) = \mathcal{F}(\boldsymbol{v}_h, \hat{\boldsymbol{v}}_h, q_h, \hat{q}_h) \;\; \forall (\boldsymbol{v}_h, \hat{\boldsymbol{v}}_h, q_h, \hat{q}_h) \in \mathbf{W}_h, \tag{6}$$

where the bilinear form $\mathcal{C}$ is defined as

$$\begin{aligned}\mathcal{C}\left((\boldsymbol{u}_h, \hat{\boldsymbol{u}}_h, p_h, \hat{p}_h), (\boldsymbol{v}_h, \hat{\boldsymbol{v}}_h, q_h, \hat{q}_h)\right) := a(\boldsymbol{u}_h, \hat{\boldsymbol{u}}_h, \boldsymbol{v}_h, \hat{\boldsymbol{v}}_h) &+ b(p_h, \hat{p}_h, \boldsymbol{v}_h, \hat{\boldsymbol{v}}_h) \\ &- b(q_h, \hat{q}_h, \boldsymbol{u}_h, \hat{\boldsymbol{u}}_h).\end{aligned}$$

4 Well posedness of the discrete problem

Here we demonstrate consistency, stability and convergence for the discrete problem. To prove stability and convergence we need boundedness of $\mathcal{C}$ and $\mathcal{F}$, positivity of $\mathcal{C}$ and inf-sup condition. The proofs of boundedness and positivity are analogous to the results shown in [7], while the inf-sup condition requires different arguments since in this work we are dealing with the fully coupled case where the reduced variables are unknown.

4.1 Consistency

We introduce the following spaces:

$$\begin{aligned}\mathbf{V} &:= \left\{\boldsymbol{v} = (\boldsymbol{v}_1, \boldsymbol{v}_2, \hat{\boldsymbol{v}}) : \boldsymbol{v}_i \in \boldsymbol{H}_{\mathrm{div}}(\Omega_i),\; \boldsymbol{v}_i \cdot \boldsymbol{n}_{\hat{\gamma}} \in L^2(\hat{\gamma}), i = 1, 2, \hat{\boldsymbol{v}} \in \boldsymbol{H}_{\mathrm{div}}(\hat{\gamma})\right\}, \\ Q &:= \left\{q = (q_1, q_2, \hat{q}) : \;\; q_i \in H^1(\Omega_i), \hat{q} \in H^1(\hat{\gamma})\right\} \subset L^2(\Omega \times \hat{\gamma}), \quad \mathbf{W} := \mathbf{V} \times Q.\end{aligned}$$

Note that the normal component $\boldsymbol{v} \cdot \boldsymbol{n}_{\hat{\gamma}}$ of a function $\boldsymbol{v} \in \mathbf{V}$ is discontinuous on $\hat{\gamma}$.

Lemma 1 (Consistency) *We consider $(\boldsymbol{u}, \hat{\boldsymbol{u}}, p, \hat{p})$ solution of problem (2) and $(\boldsymbol{u}_h, \hat{\boldsymbol{u}}_h, p_h, \hat{p}_h) \in \mathbf{W}_h$ solution of problem (6). If $(\boldsymbol{u}, \hat{\boldsymbol{u}}, p, \hat{p}) \in \mathbf{W}$, we have*

$$\mathcal{C}((\boldsymbol{u} - \boldsymbol{u}_h, \hat{\boldsymbol{u}} - \hat{\boldsymbol{u}}_h, p - p_h, \hat{p} - \hat{p}_h), (\boldsymbol{v}_h, \hat{\boldsymbol{v}}_h, q_h, \hat{q}_h)) = 0 \;\; \forall (\boldsymbol{v}_h, \hat{\boldsymbol{v}}_h, q_h, \hat{q}_h) \in \mathbf{W}_h. \tag{7}$$

Proof. Let us show that

$$\mathcal{C}((\boldsymbol{u}, \hat{\boldsymbol{u}}, p, \hat{p}), (\boldsymbol{v}_h, \hat{\boldsymbol{v}}_h, q_h, \hat{q}_h)) = \mathcal{F}(\boldsymbol{v}_h, \hat{\boldsymbol{v}}_h, q_h, \hat{q}_h) \quad \forall (\boldsymbol{v}_h, \hat{\boldsymbol{v}}_h, q_h, \hat{q}_h) \in \mathbf{W}_h.$$

Using Green's theorem in both subdomains Ω_i, $i = 1, 2$ and in $\hat{\gamma}$, we have

$$\begin{aligned}b(p, \hat{p}, \boldsymbol{v}_h, \hat{\boldsymbol{v}}_h) = \;& (\boldsymbol{v}_h, \nabla p)_\Omega - (p, \boldsymbol{v}_h \cdot \boldsymbol{n})_{\Gamma_N} - ([\![p\boldsymbol{v}_h \cdot \boldsymbol{n}_{\hat{\gamma}}]\!], 1)_{\hat{\gamma}} \\ &+ (\hat{\boldsymbol{v}}_h, \nabla_{\boldsymbol{\tau}} \hat{p})_{\hat{\gamma}} - (\hat{p}, \hat{\boldsymbol{v}}_h \cdot \boldsymbol{\tau}_{\hat{\gamma}})_{\partial_N \hat{\gamma}} + (\hat{p}, [\![\boldsymbol{v}_h \cdot \boldsymbol{n}_{\hat{\gamma}}]\!])_{\hat{\gamma}}\,.\end{aligned}$$

Hence, replacing $\eta \boldsymbol{u}+\nabla p=\boldsymbol{f}$, $\nabla\cdot\boldsymbol{u}=f$, $\hat{\eta}\hat{\boldsymbol{u}}+\nabla_{\boldsymbol{\tau}}\hat{p}=\hat{\boldsymbol{f}}$, $\nabla_{\boldsymbol{\tau}}\cdot\hat{\boldsymbol{u}}=l_{\hat{\gamma}}\tilde{f}+(\boldsymbol{u}_1-\boldsymbol{u}_2)\cdot\boldsymbol{n}_{\hat{\gamma}}$, and using the boundary conditions, we have

$$
\begin{aligned}
\mathcal{C}((\boldsymbol{u},\hat{\boldsymbol{u}},p,\hat{p}),(\boldsymbol{v}_h,\hat{\boldsymbol{v}}_h,q_h,\hat{q}_h)) &= (\boldsymbol{f}\cdot\boldsymbol{v}_h)_\Omega+(\eta_{\hat{\gamma}}\{\!\{\boldsymbol{u}\cdot\boldsymbol{n}_{\hat{\gamma}}\}\!\},\{\!\{\boldsymbol{v}_h\cdot\boldsymbol{n}_{\hat{\gamma}}\}\!\})_{\hat{\gamma}} \\
&+\xi_0\,(\eta_{\hat{\gamma}}[\![\boldsymbol{u}\cdot\boldsymbol{n}_{\hat{\gamma}}]\!],[\![\boldsymbol{v}_h\cdot\boldsymbol{n}_{\hat{\gamma}}]\!])_{\hat{\gamma}}+\left(\nu h^{-1}u_0,\boldsymbol{v}_h\cdot\boldsymbol{n}\right)_{\Gamma_D}+\left(\hat{\boldsymbol{f}},\hat{\boldsymbol{v}}_h\right)_{\hat{\gamma}} \\
&+\left(\hat{\nu}\hat{h}^{-1}\hat{u}_0,\hat{\boldsymbol{v}}_h\cdot\boldsymbol{\tau}_{\hat{\gamma}}\right)_{\partial_D\hat{\gamma}}-(p_0,\boldsymbol{v}_h\cdot\boldsymbol{n})_{\Gamma_N}-([\![p\boldsymbol{v}_h\cdot\boldsymbol{n}_{\hat{\gamma}}]\!],1)_{\hat{\gamma}}-(\hat{p}_0,\hat{\boldsymbol{v}}_h\cdot\boldsymbol{\tau}_{\hat{\gamma}})_{\partial_N\hat{\gamma}} \\
&+(\hat{p},[\![\boldsymbol{v}_h\cdot\boldsymbol{n}_{\hat{\gamma}}]\!])_{\hat{\gamma}}+(f,q_h)_\Omega-(q_h,u_0)_{\Gamma_D}-(\hat{q}_h,[\![\boldsymbol{u}\cdot\boldsymbol{n}_{\hat{\gamma}}]\!])_{\hat{\gamma}}+\left(\hat{f},\hat{q}_h\right)_{\hat{\gamma}} \\
&-(\hat{q}_h,\hat{u}_0)_{\partial_D\hat{\gamma}}+(l_{\hat{\gamma}}\{\!\{\boldsymbol{f}\cdot\boldsymbol{n}_{\hat{\gamma}}\}\!\},\{\!\{\boldsymbol{v}_h\cdot\boldsymbol{n}_{\hat{\gamma}}\}\!\})_{\hat{\gamma}}-\left(\frac{l_{\hat{\gamma}}}{4}[\![\boldsymbol{f}\cdot\boldsymbol{n}_{\hat{\gamma}}]\!],[\![\boldsymbol{v}_h\cdot\boldsymbol{n}_{\hat{\gamma}}]\!]\right)_{\hat{\gamma}}.
\end{aligned}
$$

Thanks to the algebraic identity $[\![ab]\!]=[\![a]\!]\{\!\{b\}\!\}+\{\!\{a\}\!\}[\![b]\!]$ and to the interface conditions (2b) we can write

$$
([\![p\boldsymbol{v}_h\cdot\boldsymbol{n}_{\hat{\gamma}}]\!],1)_{\hat{\gamma}}=([\![p]\!],\{\!\{\boldsymbol{v}_h\cdot\boldsymbol{n}_{\hat{\gamma}}\}\!\})_{\hat{\gamma}}+(\{\!\{p\}\!\},[\![\boldsymbol{v}_h\cdot\boldsymbol{n}_{\hat{\gamma}}]\!])_{\hat{\gamma}}=I+II
$$

where

$$
I=(\eta_{\hat{\gamma}}\{\!\{\boldsymbol{u}\cdot\boldsymbol{n}_{\hat{\gamma}}\}\!\},\{\!\{\boldsymbol{v}_h\cdot\boldsymbol{n}_{\hat{\gamma}}\}\!\})_{\hat{\gamma}}\,,\quad II=\xi_0\,(\eta_{\hat{\gamma}}[\![\boldsymbol{u}\cdot\boldsymbol{n}_{\hat{\gamma}}]\!],[\![\boldsymbol{v}_h\cdot\boldsymbol{n}_{\hat{\gamma}}]\!])_{\hat{\gamma}}+(\hat{p},[\![\boldsymbol{v}_h\cdot\boldsymbol{n}_{\hat{\gamma}}]\!])_{\hat{\gamma}}\,,
$$

so that

$$
\begin{aligned}
\mathcal{C}((\boldsymbol{u},\hat{\boldsymbol{u}},p,\hat{p}),(\boldsymbol{v}_h,\hat{\boldsymbol{v}}_h,q_h,\hat{q}_h)) &= (\boldsymbol{f},\boldsymbol{v}_h)_\Omega+\left(\nu h^{-1}u_0,\boldsymbol{v}_h\cdot\boldsymbol{n}\right)_{\Gamma_D}+\left(\hat{\boldsymbol{f}},\hat{\boldsymbol{v}}_h\right)_{\hat{\gamma}} \\
+\left(\hat{\nu}\hat{h}^{-1}\hat{u}_0,\hat{\boldsymbol{v}}_h\cdot\boldsymbol{\tau}_{\hat{\gamma}}\right)_{\partial_D\hat{\gamma}}&-(p_0,\boldsymbol{v}_h\cdot\boldsymbol{n})_{\Gamma_N}-(\hat{p}_0,\hat{\boldsymbol{v}}_h\cdot\boldsymbol{\tau}_{\hat{\gamma}})_{\partial_N\hat{\gamma}}+(f,q_h)_\Omega-(q_h,u_0)_{\Gamma_D} \\
&+\left(\hat{f}-[\![\boldsymbol{u}\cdot\boldsymbol{n}_{\hat{\gamma}}]\!],\hat{q}_h\right)_{\hat{\gamma}}-(\hat{q}_h,\hat{u}_0)_{\partial_D\hat{\gamma}}+(l_{\hat{\gamma}}\{\!\{\boldsymbol{f}\cdot\boldsymbol{n}_{\hat{\gamma}}\}\!\},\{\!\{\boldsymbol{v}_h\cdot\boldsymbol{n}_{\hat{\gamma}}\}\!\})_{\hat{\gamma}} \\
&-\left(\frac{l_{\hat{\gamma}}}{4}[\![\boldsymbol{f}\cdot\boldsymbol{n}_{\hat{\gamma}}]\!],[\![\boldsymbol{v}_h\cdot\boldsymbol{n}_{\hat{\gamma}}]\!]\right)_{\hat{\gamma}}=\mathcal{F}(\boldsymbol{v}_h,q_h).
\end{aligned}
$$

□

4.2 Boundedness and positivity

We consider the following discrete norms:

$$
\begin{aligned}
|||(\boldsymbol{v}_h,\hat{\boldsymbol{v}}_h)|||^2 &:= \|\eta^{\frac{1}{2}}\boldsymbol{v}_h\|^2_{L^2(\Omega)}+\|h^{-\frac{1}{2}}\boldsymbol{v}_h\cdot\boldsymbol{n}\|^2_{L^2(\Gamma_D)} \\
&\quad+\|\eta_{\hat{\gamma}}\{\!\{\boldsymbol{v}_h\cdot\boldsymbol{n}_{\hat{\gamma}}\}\!\}\|^2_{L^2(\hat{\gamma})}+\xi_0\|\eta_{\hat{\gamma}}[\![\boldsymbol{v}_h\cdot\boldsymbol{n}_{\hat{\gamma}}]\!]\|^2_{L^2(\hat{\gamma})} \\
&\quad+\|\hat{\eta}^{\frac{1}{2}}\hat{\boldsymbol{v}}_h\|^2_{L^2(\hat{\gamma})}+\|\hat{h}^{-\frac{1}{2}}\hat{\boldsymbol{v}}_h\cdot\boldsymbol{n}\|^2_{L^2(\partial_D\hat{\gamma})}, \qquad (8)\\
\|(\boldsymbol{v}_h,\hat{\boldsymbol{v}}_h)\|^2_{\mathbf{V}_h} &:= |||(\boldsymbol{v}_h,\hat{\boldsymbol{v}}_h)|||^2+\|\eta^{\frac{1}{2}}\nabla\cdot\boldsymbol{v}_h\|^2_{L^2(\Omega)}+\|\hat{\eta}^{\frac{1}{2}}\nabla_{\boldsymbol{\tau}}\cdot\hat{\boldsymbol{v}}_h\|^2_{L^2(\hat{\gamma})}, \\
\|(q_h,\hat{q}_h)\|^2_{Q_h} &:= \|\eta^{-\frac{1}{2}}q_h\|^2_{L^2(\Omega)}+\|\hat{\eta}^{-\frac{1}{2}}\hat{q}_h\|^2_{L^2(\hat{\gamma})},
\end{aligned}
$$

and we define the global norm as

$$
\|(\boldsymbol{v}_h,\hat{\boldsymbol{v}}_h,q_h,\hat{q}_h)\|^2_{\mathbf{W}_h}:=\|(\boldsymbol{v}_h,\hat{\boldsymbol{v}}_h)\|^2_{\mathbf{V}_h}+\|(q_h,\hat{q}_h)\|^2_{Q_h}. \qquad (9)
$$

We will also make use of the h-dependent norms $\|u\|^2_{h,\pm\frac{1}{2},\Sigma}:=\left(h^{\mp 1},u^2\right)_\Sigma$.

Lemma 2 ($\mathcal{F}$-Boundedness) *If $\xi_0 > 0$, there exists a constant C_h, depending on h and on all the problem data such that*

$$\mathcal{F}(\boldsymbol{v}_h, \hat{\boldsymbol{v}}_h, q_h, \hat{q}_h) \leq C_h \|(\boldsymbol{v}_h, \hat{\boldsymbol{v}}_h, q_h, \hat{q}_h)\|_{\mathbf{W}_h} \qquad \forall (\boldsymbol{v}_h, \hat{\boldsymbol{v}}_h, q_h, \hat{q}_h) \in \mathbf{W}_h.$$

Proof. The proof is analogous to the proof of $\mathcal{F}$-Boundedness in [7]. □

Similarly, the following properties are immediately verified, the interested reader may find the proofs in [7].

Lemma 3 (Boundedness) *The bilinear form $\mathcal{C}$ is bounded, i.e.*

$$\begin{aligned} \mathcal{C}((\boldsymbol{u}_h, \hat{\boldsymbol{u}}_h, p_h, \hat{p}_h), (\boldsymbol{v}_h, \hat{\boldsymbol{v}}_h, q_h, \hat{q}_h)) \leq \|(\boldsymbol{u}_h, \hat{\boldsymbol{u}}, p_h, \hat{p}_h)\|_{\mathbf{W}_h} \|(\boldsymbol{v}_h, \hat{\boldsymbol{v}}_h, q_h, \hat{q}_h)\|_{\mathbf{W}_h} \\ \forall (\boldsymbol{u}_h, \hat{\boldsymbol{u}}_h, p_h, \hat{p}_h), (\boldsymbol{v}_h, \hat{\boldsymbol{v}}_h, q_h, \hat{q}_h) \in \mathbf{W}_h. \end{aligned} \tag{10}$$

Lemma 4 (Positivity) *Provided that $\gamma \gtrsim 1$,*

$$\mathcal{C}((\boldsymbol{v}_h, \hat{\boldsymbol{v}}_h, q_h, \hat{q}_h), (\boldsymbol{v}_h, \hat{\boldsymbol{v}}_h, q_h, \hat{q}_h)) \geq |||(\boldsymbol{v}_h, \hat{\boldsymbol{v}}_h)|||^2 \quad \forall (\boldsymbol{v}_h, \hat{\boldsymbol{v}}_h, q_h, \hat{q}_h) \in \mathbf{W}_h. \tag{11}$$

Proof. We have

$$\mathcal{C}((\boldsymbol{v}_h, \hat{\boldsymbol{v}}_h, q_h, \hat{q}_h), (\boldsymbol{v}_h, \hat{\boldsymbol{v}}_h, q_h, \hat{q}_h)) = a(\boldsymbol{v}_h, \hat{\boldsymbol{v}}_h, \boldsymbol{v}_h, \hat{\boldsymbol{v}}_h) = |||(\boldsymbol{v}_h, \hat{\boldsymbol{v}}_h)|||^2$$

so that the lemma follows immediately. □

4.3 Inf-sup condition

Here we prove that using the extended $(\mathbb{RT}_0, \mathbb{P}_0)$ pair we can obtain an inf-sup condition under some additional assumptions on the interface $\hat{\gamma}$. Indeed, even if the standard $(\mathbb{RT}_0, \mathbb{P}_0)$ pair is inf-sup stable for the Darcy problem, this is not guaranteed in the extended "cut" case. Moreover, since we are here considering the coupled case the proof requires techniques that differ from those used in [7]. First of all, we split the domain Ω into five subregions. One is the strip of (cut) elements in $\mathcal{G}_h$, while for $i = 1, 2$ we define $\mathcal{S}_{i,h}$ as the collections of elements of $\mathcal{T}_h$ fully included in each Ω_i that have at least a vertex in common with $\mathcal{G}_h$. Finally we define $\mathcal{T}_{i,h}$ the collections of the elements fully included in each Ω_i such that they have no vertexes in common with $\mathcal{G}_h$. For an example, see Figure 3. Thus, $\mathcal{T}_h = \mathcal{T}_{1,h} \cup \mathcal{SGS}_h \cup \mathcal{T}_{2,h}$ is a disjoint union. We denote by $\hat{\gamma}_{G,i,h}$ the interface between $\mathcal{S}_{i,h}$ and $\mathcal{G}_h$ and by $\hat{\gamma}_{S,i,h}$ the interface between $\mathcal{T}_{i,h}$ and $\mathcal{S}_{i,h}$.

Hypothesis 2 *We call $N_{G,h}$ the maximum number of adjacent elements of $\mathcal{G}_h$ that have one edge in common with $\mathcal{S}_{i,h}$ for the same index i, and $N_{S,h}$ the maximum number of adjacent elements of $\mathcal{S}_{1,h}$ or $\mathcal{S}_{2,h}$ that have one edge in common with $\mathcal{T}_{1,h}$ or $\mathcal{T}_{2,h}$ respectively. We assume that there is a number M_0 independent from h such that $N_{G,h} \leq M_0$, $N_{S,h} \leq M_0$. We define $M = M_0(M_0 + 1)$.*

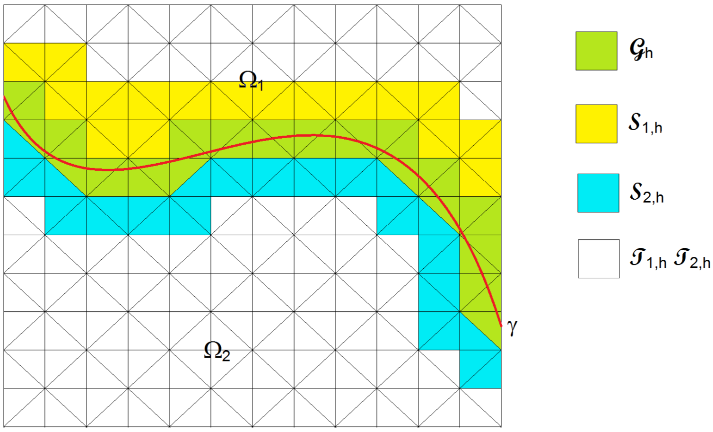

Figure 3: An example of the division of Ω in subregions.

We notice that a consequence of property H1 of the triangulation is that there is a constant $C_\rho \geq 1$ independent from h such that, calling respectively l_{max}^K and l_{min}^K the maximum and the minimum length of the edges of an element $K \in \Omega$, we have

$$l_{max}^K / l_{min}^K < C_\rho. \tag{12}$$

For each $K \in \mathcal{G}_h$, let E_K be the only edge of K that is not cut by $\hat{\gamma}$. For a given index $i = 1, 2$, thanks to Hypothesis 3, there are only two cases: either $E_K \cap \Omega_i = \emptyset$, or $E_K \subset \hat{\gamma}_{G,i,h}$. In the first case, the sub-element K_i is a triangle: we say that K_i is of type T and write $K_i \sim T$. In the other case, the sub-element K_i is a quadrangle: we say that K_i is of type Q and write $K_i \sim Q$, see Figure 4.

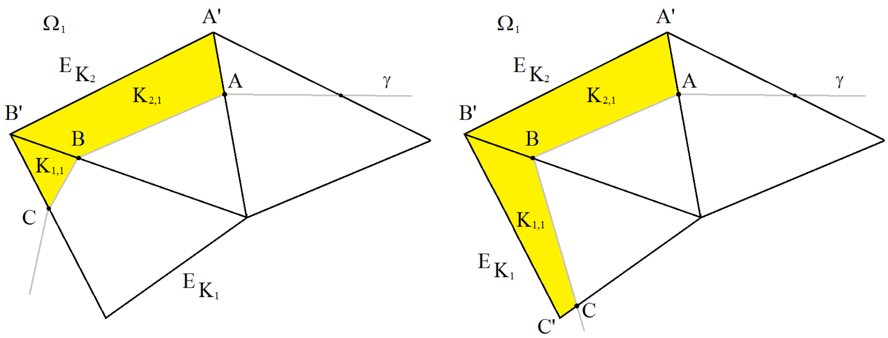

Figure 4: Two elements $K_j \in \mathcal{G}_h$, $j = 1, 2$, cut by an interface $\hat{\gamma} = ABC$. Up: $K_1 \sim T$ ($K_{1,1}$ is a triangle, E_{K_1} is outside Ω_1), $K_2 \sim Q$ ($K_{2,1}$ is a quadrangle, E_{K_2} is on $\hat{\gamma}_{1,h} \subset \Omega_1$). Down: $K_1, K_2 \sim Q$ ($K_{j,1}$ is a quadrangle, E_{K_j} is on $\hat{\gamma}_{1,h} \subset \Omega_i$, $j = 1, 2$).

Hypothesis 3 *For every K_1, K_2 adjacent elements in $\mathcal{T}_h$, if the edge between K_1 and K_2 is not cut by $\hat{\gamma}$, then either $K_1 \notin \mathcal{G}_h$ or $K_2 \notin \mathcal{G}_h$.*

For a fixed $\hat{\gamma}$, it can be verified that it is always possible to build a mesh that satisfy Hypothesis 3.

Hypothesis 4 *Let K_1, K_2 be two adjacent elements in $\mathcal{G}_h$ (i.e. sharing an edge E). There exist two constants $c, C > 0$, dependent on $\hat{\gamma}$ only, such that*

$$|K_{1,i}| \leq C|K_{2,i}| \text{ if } K_{1,i} \sim T \text{ and } K_{2,i} \sim Q; \tag{13}$$

$$c|K_{1,i}| \leq |K_{2,i}| \leq C|K_{1,i}| \text{ if } K_{1,j}, K_{2,j} \sim Q. \tag{14}$$

Lemma 4.1 *Hypothesis 4 is satisfied if the ratio between the curvature radius ρ of $\hat{\gamma}$ and the mesh size h is large enough, i.e. $\rho \geq C_{\hat{\gamma}} h$ with $C_{\hat{\gamma}}$ a positive constant. Hence, it holds for a sufficiently refined mesh.*

Proof. See [7]. □

Let K be an elements in $\mathcal{G}_h$. We call $\boldsymbol{\phi}_r$ the r^{th} basis function of $\mathbb{RT}_0(K)$ for $r = 1, 2, 3$. We indicate with $\boldsymbol{\phi}_3$ the function corresponding to the *d.o.f.* relative to the edge not cut by $\hat{\gamma}$. Also, we define $c_r = \boldsymbol{\phi}_r \cdot \boldsymbol{n}_{\hat{\gamma}}$ and we recall that c_r is a constant because $\boldsymbol{\phi}_r \in \mathbb{RT}_0(K)$. Thanks to Property H2 we have that $c_r \neq 0$ for every r. Considering that $\boldsymbol{\phi}_r$, along an edge E_s with $r \neq s$, is parallel to the edge (because $\boldsymbol{\phi}_r \cdot \boldsymbol{n}_{E_s} = 0$) and that its versus is directed towards the edge E_r, we obtain that $c_1 c_3 < 0$ and $c_2 c_3 < 0$, see Figure 5, and hence $c_1 - c_3 \neq 0$, $c_2 - c_3 \neq 0$ and $\frac{|c_j|}{|c_j - c_3|} \leq 1$ for every $K \in \mathcal{G}_h$ and $j = 1, 2$.

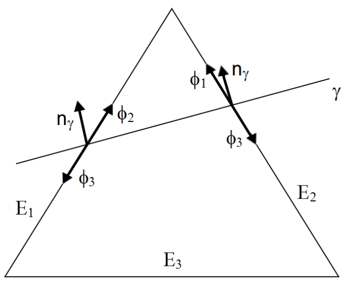

Figure 5: Considering that $c_r = \boldsymbol{\phi}_r \cdot \boldsymbol{n}_{\hat{\gamma}}$ is constant along $\hat{\gamma}$ for $r = 1, 2, 3$, from the intersection between E_1 and $\hat{\gamma}$ we obtain that $c_2 c_3 < 0$, and form the intersection between E_2 and $\hat{\gamma}$ that $c_1 c_3 < 0$.

Hypothesis 5 *There exists a constant $d_{\boldsymbol{\phi}}$ not depending on h such that*

$$d_{\boldsymbol{\phi}} \geq \max_{K_j \in \mathcal{G}_h} \frac{|c_i - c_3|}{|c_j - c_3|} \quad \text{and} \quad d_{\boldsymbol{\phi}} \geq \max_{K_j \in \mathcal{G}_h} \frac{|c_i - c_j|}{|c_j - c_3|}, \tag{15}$$

for both $(i, j) = (1, 2)$ and $(i, j) = (2, 1)$.

We notice that $\frac{|c_i-c_3|}{|c_j-c_3|} \to \infty$ and $\frac{|c_i-c_j|}{|c_j-c_3|} \to \infty$ if and only if $c_i \to 1$ and $c_j, c_3 \to 0$, that is if and only if the angle between $\hat{\gamma}$ and E_i tends to 0. Thus Hypothesis 5 is equivalent to ask that there is a minimum angle $\alpha > 0$, such that $\hat{\gamma}$ intersects $E_{K,1}$ and $E_{K,2}$ with angle greater than α for every $K \in \mathcal{G}_h$. This condition does not represent a constraint for practical cases. We will also need the following auxiliary lemma about the surjectivity of the divergence operator onto L^2.

Lemma 5 *Let Ω be a Lipschitz domain, and let $\hat{\gamma} \subset \partial\Omega$, $\hat{\gamma} \neq \partial\Omega$, be a Lipschitz subset of its boundary. For any $q \in L^2(\Omega)$, there exists $\boldsymbol{v} \in H^1(\Omega)$ such that*

$$\nabla \cdot \boldsymbol{v} = q, \quad \boldsymbol{v}_{|\hat{\gamma}} = \mathbf{0}, \quad \|\boldsymbol{v}\|_{H^1(\Omega)} \lesssim \|q\|_{L^2(\Omega)}.$$

Proof. We proceed as in [7]. If $q \in L^2_0(\Omega) = \{f \in L^2(\Omega) : (f,1)_\Omega = 0\}$ and $\hat{\gamma} = \partial\Omega$, this is a well known result [15]. To deal with the general case in which $\hat{\gamma}$ is only part of the boundary, consider any lifting $\boldsymbol{h} \in H^1(\Omega)$ of a smooth boundary datum satisfying $\boldsymbol{h}_{|\hat{\gamma}} = \mathbf{0}$, $(\boldsymbol{h} \cdot \boldsymbol{n}, 1)_{\partial\Omega} \neq 0$. By normalization, we can require $(\nabla \cdot \boldsymbol{h}, 1)_\Omega = 1$. Let $\bar{q} = (q,1)_\Omega \in \mathbb{R}$, and consider $q_0 = q - \bar{q}(\nabla \cdot \boldsymbol{h})$. We have $q_0 \in L^2_0(\Omega)$. Then, there exists $\boldsymbol{v}_0 \in H^1(\Omega)$ such that

$$\nabla \cdot \boldsymbol{v}_0 = q_0, \quad \boldsymbol{v}_{0|\partial\Omega} = \mathbf{0}, \quad \|\boldsymbol{v}_0\|_{H^1(\Omega)} \lesssim \|q_0\|_{L^2(\Omega)}.$$

Let $\boldsymbol{v} = \boldsymbol{v}_0 + \bar{q}\boldsymbol{h}$. Since $\nabla \cdot \boldsymbol{v} = q_0 + \bar{q}(\nabla \cdot \boldsymbol{h}) = q$, and $\|\boldsymbol{v}\|_{H^1(\Omega)} \leq \|\boldsymbol{v}_0\|_{H^1(\Omega)} + |\bar{q}|\|\boldsymbol{h}\|_{H^1(\Omega)} \lesssim \|q_0\|_{L^2(\Omega)} + |\bar{q}| \lesssim \|q\|_{L^2(\Omega)}$ the proof is concluded. □

We are now in the position to prove the inf-sup condition for the coupled problem.

Theorem 4.1 (inf-sup condition) *For any $(p_h, \hat{p}_h) \in Q_h$, there exist $(\boldsymbol{v}_{p,h}, \hat{\boldsymbol{v}}_{p,h}) \in \mathbf{V}_h$ and $M_{\hat{\gamma}} > 0$ independent on h, such that $\boldsymbol{v}_{p,h} \cdot \boldsymbol{n}_{\Gamma_D} = 0$, $\hat{\boldsymbol{v}}_{p,h} \cdot \boldsymbol{n}_{\partial_D\hat{\gamma}} = 0$ and*

$$b(p_h, \hat{p}_h, \boldsymbol{v}_{p,h}, \hat{\boldsymbol{v}}_{p,h}) \gtrsim \|\eta^{-\frac{1}{2}} p_h\|^2_{L^2(\Omega)} + \|\hat{\eta}^{-\frac{1}{2}} \hat{p}_h\|^2_{L^2(\hat{\gamma})}, \tag{16}$$

$$\|(\boldsymbol{v}_{p,h}, \hat{\boldsymbol{v}}_{p,h})\|_{\mathbf{V}_h} \leq M_{\hat{\gamma}} \|\eta^{-\frac{1}{2}} p_h\|^2_{L^2(\Omega)} + M_{\hat{\gamma}} \|\hat{\eta}^{-\frac{1}{2}} \hat{p}_h\|^2_{L^2(\hat{\gamma})}. \tag{17}$$

Proof. To build the desired velocity we consider the subdomains $\mathcal{T}_{1,h}$, $\mathcal{T}_{2,h}$, $\mathcal{S}_{1,h} \cup \mathcal{G}_h \cup \mathcal{S}_{2,h}$ separately, and the fracture $\hat{\gamma}$. Thanks to the bilinearity of b, it is sufficient to show the inf-sup inequalities are verified locally into those subdomains. We indicate by $\mathcal{SGS}_h = \mathcal{S}_{1,h} \cup \mathcal{G}_h \cup \mathcal{S}_{2,h}$. We divide the proof in three parts: the first for the fracture $\hat{\gamma}$, the second for $\mathcal{T}_{1,h}$ and $\mathcal{T}_{2,h}$, and the third for $\mathcal{SGS}_h$.

Part 1 - Fracture $\hat{\gamma}$. We choose a piecewise constant functions $\hat{g}_h \in L^2(\hat{\gamma})$ such that $\hat{g}_{h|\hat{K}_i} = \hat{\eta}_i^{-1} \hat{p}_{h|\hat{K}_i}$ on each $\hat{K}$, and we consider $\partial_N\hat{\gamma} \cap \hat{\mathcal{T}}_{i,h} \neq \emptyset$. Then thanks to Lemma 5, there exists $\bar{\hat{\boldsymbol{v}}} \in H^1(\hat{\gamma})$ such that $\bar{\hat{\boldsymbol{v}}} = \mathbf{0}$ on $\partial_D\hat{\gamma}$, $\nabla_{\boldsymbol{\tau}} \cdot \bar{\hat{\boldsymbol{v}}} = -\hat{g}_h$, $\|\bar{\hat{\boldsymbol{v}}}\|_{H^1(\hat{\gamma})} \lesssim \|\hat{g}_h\|_{L^2(\hat{\gamma})}$. We have $\|\hat{\eta}_i^{\frac{1}{2}} \bar{\hat{\boldsymbol{v}}}_h\|_{H^1(\hat{\mathcal{T}}_h)} \lesssim \|\hat{\eta}_i^{-\frac{1}{2}} \hat{p}_h\|_{L^2(\hat{\mathcal{T}}_h)}$, $\bar{\hat{\boldsymbol{v}}}_h \cdot \boldsymbol{n} = 0$ on $\partial\hat{\mathcal{T}}_h \cap \partial_D\hat{\gamma}$, and

$$b(p_h, \hat{p}_h, \mathbf{0}, \bar{\hat{\boldsymbol{v}}}_h) = -\left(\hat{p}_h, \nabla_{\boldsymbol{\tau}} \cdot \bar{\hat{\boldsymbol{v}}}_h\right)_{\hat{\gamma}} = -\left(\hat{p}_h, \nabla_{\boldsymbol{\tau}} \cdot \bar{\hat{\boldsymbol{v}}}\right)_{\hat{\gamma}} = \|\hat{\eta}^{-\frac{1}{2}} \hat{p}_h\|^2_{L^2(\hat{\gamma})}.$$

Part 2 - Subdomains $\mathcal{T}_{1,h}$, $\mathcal{T}_{2,h}$. Thanks to Part 1, now it is sufficient to prove that for any $(p_h, \hat{p}_h) \in Q_h$, there exists $(\boldsymbol{v}_{p,h}, 0) \in \mathbf{V}_h$ such that $\boldsymbol{v}_{p,h} \cdot \boldsymbol{n}_{\Gamma_D} = 0$ and

$$b(p_h, \hat{p}_h, \boldsymbol{v}_{p,h}, \mathbf{0}) \gtrsim \|\eta^{-\frac{1}{2}} p_h\|^2_{L^2(\Omega)}, \qquad \|(\boldsymbol{v}_{p,h}, \mathbf{0})\|_{\mathbf{V}_h} \lesssim \|\eta^{-\frac{1}{2}} p_h\|^2_{L^2(\Omega)}.$$

We need the piecewise constant functions $g_{i,h} \in L^2(\Omega_i)$ such that $g_{i,h|K_i} = \eta_i^{-1} p_{i,h|K_i}$ on each K. For the sake of simplicity, we will consider the case in which $\Gamma_N \cap \mathcal{T}_{i,h} \neq \emptyset$. Thanks to Lemma 5, there exists $\bar{\boldsymbol{v}}_i \in H^1(\Omega_i)$ such that $\bar{\boldsymbol{v}}_i = \mathbf{0}$ on $\partial\mathcal{T}_{i,h}\backslash\Gamma_N$, $\nabla \cdot \bar{\boldsymbol{v}}_i = -g_{i,h}$, $\|\bar{\boldsymbol{v}}_i\|_{H^1(\mathcal{T}_{i,h})} \lesssim \|g_{i,h}\|_{L^2(\mathcal{T}_{i,h})}$. Note that $\bar{\boldsymbol{v}}_i = \mathbf{0}$ on $\hat{\gamma}_{S,i,h} \subset \partial\mathcal{T}_{i,h}$ and $\|\eta_i^{\frac{1}{2}}\bar{\boldsymbol{v}}_i\|_{H^1(\mathcal{T}_{i,h})} \lesssim \|\eta_i^{-\frac{1}{2}} p_{i,h}\|_{L^2(\mathcal{T}_{i,h})}$, η_i being constant on $\mathcal{T}_{i,h}$. Thanks to the continuous $\boldsymbol{H}_{\text{div}}(\mathcal{T}_{i,h})$-conformal $\mathbb{RT}_0$ interpolant $\boldsymbol{I}_{i,h}$ such that $\left((\boldsymbol{I} - \boldsymbol{I}_{i,h})\bar{\boldsymbol{v}}_i, \boldsymbol{n}_E\right)_E = 0$ on all edges E of all elements $K \in \mathcal{T}_{i,h}$, let us define $\bar{\boldsymbol{v}}_{i,h}$, such that $(\bar{\boldsymbol{v}}_{i,h}, 0) \in \mathbf{V}_h$, as the extension of $I_{i,h}\bar{\boldsymbol{v}}_i$ by zero on $\Omega\backslash\mathcal{T}_{i,h}$. We have $\|\eta_i^{\frac{1}{2}}\bar{\boldsymbol{v}}_{i,h}\|_{H^1(\mathcal{T}_{i,h})} \lesssim \|\eta_i^{-\frac{1}{2}} p_{i,h}\|_{L^2(\mathcal{T}_{i,h})}$, $\bar{\boldsymbol{v}}_{i,h} \cdot \boldsymbol{n} = 0$ on $\partial\mathcal{T}_{i,h} \cap \Gamma_D$, and

$$\begin{aligned}
b(p_h, \hat{p}_h, \bar{\boldsymbol{v}}_{i,h}, \mathbf{0}) &= -\left(p_{i,h}, \nabla \cdot \bar{\boldsymbol{v}}_{i,h}\right)_{\mathcal{T}_{i,h}} + (\hat{p}_h, [\![\widetilde{\boldsymbol{v}}_{i,K,h} \cdot \boldsymbol{n}_{\hat{\gamma}}]\!])_{\hat{\gamma}\cap\mathcal{T}_{i,h}} \\
&= -\left(p_{i,h}, \nabla \cdot \bar{\boldsymbol{v}}_i\right)_{\mathcal{T}_{i,h}} = \|\eta^{-\frac{1}{2}} p_h\|^2_{L^2(\mathcal{T}_{i,h})}
\end{aligned}$$

considering that $\hat{\gamma} \cap \mathcal{T}_{i,h} = \emptyset$.

Part 3 - Subdomain $\mathcal{S}_{1,h} \cup \mathcal{G}_h \cup \mathcal{S}_{2,h}$. Thanks to the results obtained in Part 1 and Part 2, now it is sufficient to find $\widetilde{\boldsymbol{v}}_h \in \mathbf{V}_h$ such that $\text{supp}(\widetilde{\boldsymbol{v}}_h) \subset \mathcal{SGS}_h$, with $\widetilde{\boldsymbol{v}}_h \cdot \boldsymbol{n}_{\Gamma_D} = 0$, and that satisfies the two inequalities:

$$b(p_h, \widetilde{\boldsymbol{v}}_h) \gtrsim \|\eta^{-\frac{1}{2}} p_h\|^2_{L^2(\mathcal{SGS}_h)}, \quad \|\eta_i^{\frac{1}{2}} \widetilde{\boldsymbol{v}}_h\|_{\mathbf{V}_h} \lesssim \|\eta_i^{-\frac{1}{2}} p_{i,h}\|_{L^2(\mathcal{SGS}_h)}. \tag{18}$$

We now give a special construction for such $\widetilde{\boldsymbol{v}}_h$ on $\mathcal{G}_h$ and on $\mathcal{S}_{i,h}$, $i = 1, 2$. In particular we build $\widetilde{\boldsymbol{v}}_h \in H^1(\Omega)$, and by the trace inequality, for this $\widetilde{\boldsymbol{v}}_h$ we have $\|\eta_{\hat{\gamma}} \{\!\{\widetilde{\boldsymbol{v}}_h \cdot \boldsymbol{n}_{\hat{\gamma}}\}\!\}\|^2_{L^2(\hat{\gamma})} + \xi_0 \|\eta_{\hat{\gamma}} [\![\widetilde{\boldsymbol{v}}_h \cdot \boldsymbol{n}_{\hat{\gamma}}]\!]\|^2_{L^2(\hat{\gamma})} \lesssim \|\eta_i^{\frac{1}{2}} \widetilde{\boldsymbol{v}}_h\|_{H^1(\mathcal{G}_h)}$, and therefore, by recalling (8), the inequalities (18) are satisfied if:

$$b(p_h, \widetilde{\boldsymbol{v}}_h) \gtrsim \|\eta^{-\frac{1}{2}} p_h\|^2_{L^2(\mathcal{SGS}_h)}, \quad \|\eta_i^{\frac{1}{2}} \widetilde{\boldsymbol{v}}_h\|_{H^1(\mathcal{SGS}_h)} \lesssim \|\eta_i^{-\frac{1}{2}} p_{i,h}\|_{L^2(\mathcal{SGS}_h)}. \tag{19}$$

Part 3a - Subdomain $\mathcal{G}_h$. We consider $\mathcal{G}_h$ first. We indicate with $N_{\mathcal{G}_h}$ the number of elements of $\mathcal{G}_h$. We enumerate the elements of $\mathcal{G}_h$ from 0 to $N_{\mathcal{G}_h} - 1$ such that K_0 is one of the elements in $\mathcal{G}_h$ that has an edge in common with $\partial\Omega$, and K_j has an edge in common with K_{j-1}. We call $\widetilde{\boldsymbol{v}}_{K_j,h}$ the restriction of $\widetilde{\boldsymbol{v}}_h$ on an element K_j. Moreover, we call $K_{j,i}$ the part of element K_j contained in Ω_i.

Every element $K_j \in \mathcal{G}_h$, it is divided by $\hat{\gamma}$ in two elements $K_{j,1} \in \Omega_1$ and $K_{j,2} \in \Omega_2$. We want to build $\widetilde{\boldsymbol{v}}_{K_j,h}$ such that $\widetilde{\boldsymbol{v}}_{K_j,h}|_{K_{j,i}} = \widetilde{\boldsymbol{v}}_{K_{j,i},h}|_{K_{j,i}}$, where $\widetilde{\boldsymbol{v}}_{K_{j,i},h}$ for $i = 1, 2$ are two different functions belonging to $\mathbb{RT}_0(K_j)$, and such that

$$b(p_h, \hat{p}_h, \widetilde{\boldsymbol{v}}_{K_j,h}, \mathbf{0}) \gtrsim \|\eta^{-\frac{1}{2}} p_h\|^2_{L^2(K_j)}, \quad \|\eta^{\frac{1}{2}} \widetilde{\boldsymbol{v}}_{K_j,h}\|^2_{H^1(K_j)} \lesssim \|\eta^{-\frac{1}{2}} p_h\|^2_{L^2(\mathcal{SGS}_h)}. \tag{20}$$

We start considering the first inequality. If we find a $\widetilde{\boldsymbol{v}}_{K_j,h}$ such that $-\nabla \cdot \widetilde{\boldsymbol{v}}_{K_j,h} \gtrsim \eta^{-1} p_h$, $[\![\widetilde{\boldsymbol{v}}_{K_j,h} \cdot \boldsymbol{n}_{\hat{\gamma}}]\!] = 0$ on K_j, we obtain

$$\begin{aligned}
b(p_h, \hat{p}_h, \widetilde{\boldsymbol{v}}_{K_j,h}, \mathbf{0}) &= -\left(p_h, \nabla \cdot \widetilde{\boldsymbol{v}}_{K_j,h}\right)_{K_j} + \left(\hat{p}_h, [\![\widetilde{\boldsymbol{v}}_{K_j,h} \cdot \boldsymbol{n}_{\hat{\gamma}}]\!]\right)_{\hat{\gamma}_{K_j}} \\
&\gtrsim \left(\eta^{-1} p_h, p_h\right)_{K_j} = \|\eta^{-\frac{1}{2}} p_h\|^2_{L^2(K_j)}
\end{aligned} \tag{21}$$

and the desired condition is satisfied. For $i = 1, 2$ we consider $\widetilde{\boldsymbol{v}}_{K_{j,i},h} = m_{j,i,1}\boldsymbol{\phi}_{j,1} + m_{j,i,2}\boldsymbol{\phi}_{j,2} + m_{j,i,3}\boldsymbol{\phi}_{j,3}$ where $\boldsymbol{\phi}_{j,r}$ is the basis function corresponding to the degrees of freedom $m_{j,i,r}$ of K_j: in this way, finding $\widetilde{\boldsymbol{v}}_{K_{j,i},h}$ is equivalent to finding the values of $m_{j,i,r}$ for $r = 1, 2, 3$. To obtain $-\nabla \cdot \widetilde{\boldsymbol{v}}_{K_j,h} \gtrsim \eta^{-\frac{1}{2}} p_h$ on K_j it is sufficient to have

$-\nabla_i \cdot \widetilde{\boldsymbol{v}}_{K_{j,i},h} \gtrsim \eta_i^{-1} p_{i,h}$ on $K_{j,i}$. We can use the divergence theorem on K_j and obtain that the previous condition is equivalent to

$$\eta_i^{-1} p_{i,h} \leq -\nabla \cdot \widetilde{\boldsymbol{v}}_{K_{j,i},h} = -\frac{1}{|K_j|}\left(\nabla \cdot \widetilde{\boldsymbol{v}}_{K_{j,i},h}, 1\right)_{K_j} = -\frac{1}{|K_j|}\left(\widetilde{\boldsymbol{v}}_{K_{j,i},h} \cdot \boldsymbol{n}_{\partial K_j}, 1\right)_{\partial K_j}$$

that is $\left(\widetilde{\boldsymbol{v}}_{K_{j,i},h} \cdot \boldsymbol{n}_{\partial K_j}, 1\right)_{\partial K_j} \geq |K_j| \eta_i^{-1} p_{i,h}$. We call $E_{j,r}$ the edge of K_j corresponding to the degree of freedom $m_{j,i,r}$, and $l_{j,r}$ its length. Thanks to Hypothesis 3, every K_j has one and only one edge in common with $\partial\mathcal{S}_{1,h}$ or $\partial\mathcal{S}_{2,h}$, and we enumerate the edges of every K_j so that this edge is $E_{j,3}$. We call $\boldsymbol{n}_{E_{j,r}}$ the external normal on $E_{j,r}$; moreover we recall that $\boldsymbol{\phi}_{j,r} \cdot \boldsymbol{l}$ is constant along any line $\boldsymbol{l}$ (because $\boldsymbol{\phi}_{j,r}$ is a basis function of $\mathbb{RT}_0(K_j)$), and that in particular $\phi_{j,r} \cdot \boldsymbol{n}_{E_{j,k}} = \delta_{r,k}$ for r and $k = 1,2,3$. Hence we obtain

$$\begin{aligned} -\left(\widetilde{\boldsymbol{v}}_{K_{j,i},h} \cdot \boldsymbol{n}_{\partial K_j}, 1\right)_{\partial K_j} &= -\sum_{r=1}^{3} \int_{E_{j,r}} \left(m_{j,i,1}\boldsymbol{\phi}_{j,1} + m_{j,i,2}\boldsymbol{\phi}_{j,i,2} + m_{j,i,3}\boldsymbol{\phi}_{j,i,3}\right) \cdot \boldsymbol{n}_{E_{j,r}} \\ &= -m_{j,i,1} l_{j,1} - m_{j,i,2} l_{j,2} - m_{j,i,3} l_{j,3}, \end{aligned}$$

with $l_r \neq 0$ for every r. The first condition is then equivalent to

$$-m_{j,i,1} l_{j,1} - m_{j,i,2} l_{j,2} - m_{j,i,3} l_{j,3} \gtrsim \eta_i^{-1} p_{i,h} |K_j|.$$

To have $[\![\widetilde{\boldsymbol{v}}_{K_j,h} \cdot \boldsymbol{n}_{\hat{\gamma}}]\!] = 0$ we set $\widetilde{\boldsymbol{v}}_{K_{j,i},h} \cdot \boldsymbol{n}_{\hat{\gamma}} = s_j$, $i = 1,2$, for some constant s_j to be decided later. Using again $\widetilde{\boldsymbol{v}}_{K_{j,i},h} = m_{j,i,1}\boldsymbol{\phi}_{j,1} + m_{j,i,2}\boldsymbol{\phi}_{j,2} + m_{j,i,3}\boldsymbol{\phi}_{j,3}$ and recalling that $c_r = \boldsymbol{\phi}_r \cdot \boldsymbol{n}_{\hat{\gamma}}$, we obtain

$$m_{j,i,1} c_{j,1} + m_{j,i,2} c_{j,2} + m_{j,i,3} c_{j,3} = s_j \quad i = 1,2.$$

It is important to recall that with $c_r \neq 0$ for every r, $c_{j,1}c_{j,3} < 0$ and $c_{j,2}c_{j,3} < 0$. Hence we obtain the following system for $i = 1,2$ and $j = 0, \ldots, N_{\mathcal{G}_h} - 1$

$$\begin{cases} -m_{j,i,1} l_{j,1} - m_{j,i,2} l_{j,2} - m_{j,i,3} l_{j,3} \gtrsim \eta_i^{-1} p_{i,h} |K_j| \\ m_{j,i,1} c_{j,1} + m_{j,i,2} c_{j,2} + m_{j,i,3} c_{j,3} = s_j \end{cases}.$$

Now we decide how to enumerate the edges of every K_j. We have already decided that $E_{j,3}$ is the only edge of K_j not cut by $\hat{\gamma}$. Moreover, we have chosen K_0 such that it has an edge in common with $\partial\Omega$, that we denote as $E_{0,1}$; hence $E_{0,2}$ is the other edge of K_j that intersect $\hat{\gamma}$. Then, we enumerate the edges $E_{j,1}$, $E_{j,2}$ for $j \geq 1$ such that $E_{j,i,1} = E_{j-1,i,2}$. For $i = 1,2$, we want to construct the velocity $\widetilde{\boldsymbol{v}}_{K_{j,i},h}$ first for $j = 0$, then on $j = 1$, and so on for all $K \in \mathcal{G}_h$. Setting $m_{0,i,1} = 0$ we find $m_{0,i,2}$ and $m_{0,i,3}$ such that

$$-m_{0,i,2} l_{0,2} - m_{0,i,3} l_{0,3} = \eta_i^{-1} p_{j,i,h} |K_0|, \quad m_{0,i,2} c_{0,2} + m_{0,i,3} c_{0,3} = s_0,$$

that is $m_{0,i,2} = a_{0,2} \eta_i^{-1} p_{i,h_0} |K_0| + q_{0,2} s_0$ and $m_{0,i,3} = a_{0,3} \eta_i^{-1} p_{i,h_0} |K_0| + q_{0,3} s_0$, where

$$\begin{aligned} a_{0,2} &= \frac{c_{0,3}}{l_{0,3}c_{0,2} - l_{0,2}c_{0,3}}, & a_{0,3} &= \frac{-c_{0,2}}{l_{0,3}c_{0,2} - l_{0,2}c_{0,3}}, \\ q_{0,2} &= \frac{l_{0,3}}{l_{0,3}c_{0,2} - l_{0,2}c_{0,3}}, & q_{0,3} &= \frac{-l_{0,2}}{l_{0,3}c_{0,2} - l_{0,2}c_{0,3}}. \end{aligned}$$

The system is not singular since $l_{0,1} > 0$, $l_{0,2} > 0$ and $c_2 c_3 < 0$, thus $l_{0,3}c_{0,2}$ and $-l_{0,2}c_{0,3}$ are different from 0 and have the same sign, and hence $l_{0,3}c_{0,2} - l_{0,2}c_{0,3} \neq 0$. For all the other K_j, to maintain the continuity on $E_{j,1} = E_{j-1,2}$, we must set $m_{j,i,1} = -m_{j-1,i,2}$, and hence we find $m_{j,i,2}$ and $m_{j,i,3}$ such that

$$\begin{cases} -m_{j,i,2}l_{j,2} - m_{j,i,3}l_{j,3} = \eta_i^{-1}p_{j,i,h}|K_j| - m_{j-1,i,2}l_{j,1} \\ m_{j,i,2}c_{j,2} + m_{j,i,3}c_{j,3} = m_{j-1,i,2}c_{j,1} + s_j \end{cases}.$$

The solution of the previous system is $m_{j,i,2} = a_{j,2}\eta_i^{-1}p_{j,i,h}|K_j| + b_2 m_{j-1,i,2} + q_{j,2}s_j$ and $m_{j,i,3} = a_{j,3}\eta_i^{-1}p_{j,i,h}|K_j| + b_3 m_{j-1,i,2} + q_{j,3}s_j$, where

$$a_{j,2} = \frac{c_{j,3}}{l_{j,3}c_{j,2} - l_{j,2}c_{j,3}}, \quad a_{j,3} = \frac{-c_{j,2}}{l_{j,3}c_{j,2} - l_{j,2}c_{j,3}}, \quad b_{j,2} = \frac{l_{j,3}c_{j,1} - c_{j,3}l_{j,1}}{l_{j,3}c_{j,2} - l_{j,2}c_{j,3}},$$
$$b_{j,3} = \frac{-l_{j,2}c_{j,1} - c_{j,2}l_{j,1}}{l_{j,3}c_{j,2} - l_{j,2}c_{j,3}}, \quad q_{j,2} = \frac{l_{j,3}}{l_{j,3}c_{j,2} - l_{j,2}c_{j,3}}, \quad q_{j,3} = \frac{-l_{j,2}}{l_{j,3}c_{j,2} - l_{j,2}c_{j,3}}.$$

Again, the system is not singular for every K_j because, like in K_0, for every j we have $l_{j,3}c_{j,2} - l_{j,2}c_{j,3} \neq 0$. Therefore, on every K_j, independently from the choice of s_j, we have built a function $\widetilde{\boldsymbol{v}}_{K_j,h}$, with $\widetilde{\boldsymbol{v}}_{K_{j,i},h} = m_{j,i,1}\boldsymbol{\phi}_{j,1} + m_{j,i,2}\boldsymbol{\phi}_{j,2} + m_{j,i,3}\boldsymbol{\phi}_{j,3}$, that satisfies the first inequality in 20. We still need to show that, if we choose s_j in an appropriate way, we have that $\widetilde{\boldsymbol{v}}_{K_j,h}$ satisfies $\|\eta_i^{\frac{1}{2}}\widetilde{\boldsymbol{v}}_h\|_{H^1(\mathcal{G}_h)} \lesssim \|\eta^{-\frac{1}{2}}p_h\|_{L^2(\mathcal{SGS}_h)}$ for $i = 1, 2$. We observe that

$$|a_{j,2}| = \frac{|c_{j,3}|}{|l_{j,3}c_{j,2} - l_{j,2}c_{j,3}|} \leq \frac{1}{l_{j,min}} \frac{|c_{j,3}|}{|c_{j,2} - c_{j,3}|} \leq \frac{1}{l_{j,min}}$$

where $l_{j,min}$ is the length of the shorter edge of K_j (we used the fact that $c_{j,2}c_{j,3} < 0$). In the same way we obtain $|a_{j,3}| \leq \frac{1}{l_{j,min}}$ for $r = 2, 3$. We observe also that

$$|b_{j,2}| = \frac{|l_{j,3}c_{j,1} - l_{j,1}c_{j,3}|}{|l_{j,3}c_{j,2} - l_{j,2}c_{j,3}|} \leq \frac{l_{j,max}}{l_{j,min}} \frac{|c_{j,1} - c_{j,3}|}{|c_{j,2} - c_{j,3}|} \leq C_\rho \frac{|c_{j,1} - c_{j,3}|}{|c_{j,2} - c_{j,3}|} \leq C_\rho d_{\boldsymbol{\phi}},$$

by (12) and (15), and analogously $|b_{j,3}| \leq C_\rho d_{\boldsymbol{\phi}}$, $|q_{j,2}||c_{j,2}| \leq C_\rho$, $|q_{j,3}||c_{j,2}| \leq C_\rho$.

Now, we divide the elements of $\mathcal{G}_h$ into groups. Starting from K_0 every group G_z for $z = 1, ..., N_{G,h}$ is made by the two successive elements K_j after G_{z-1} and by additional successive elements until, between the third and the last element of G_z, there is at least one element K_{j_1} that has the edge $E_{j-1,3}$ in common with $\mathcal{S}_{1,h}$ and one element K_{j_2} that has $E_{j-2,3}$ in common with $\mathcal{S}_{2,h}$. We indicate with (z, t) the index, in the global enumeration K_j, of the t^{th} element of the z^{th} group, thus $K_{(z,t)}$ are the elements of G_z for $t = 0, ..., N_{G_z} - 1$. We observe that G_z is made by the first two elements, followed by a set of adjacent elements that have all one edge in common with $\mathcal{S}_{i,h}$ for the same index i, apart from the last element. Hence by construction we have $N_{G_z} \leq M_0 + 3 \leq M$. We observe that with this construction $E_{(z,N_{G_z}-2),3}$ and $E_{(z,N_{G_z}-1),3}$ are in common with $\mathcal{S}_{i,h}$ and $\mathcal{S}_{j,h}$ respectively $i \neq j$. We call H_i the set of all the edges $E_{(z,N_{G_z}-2),3}$ or $E_{(z,N_{G_z}-1),3}$ that are in Ω_i. Fixed an index i, we have $H_i \in \hat{\gamma}_{G,i,h}$ and we observe that between two edges of H_i there can be at most M_0 edges that are not in H_i. See Figure 6 for an example. We chose to take $s_{(z,0)}$ such that $|m_{(z,0),1,2}| = 0$ and $s_{(z,1)}$ such that

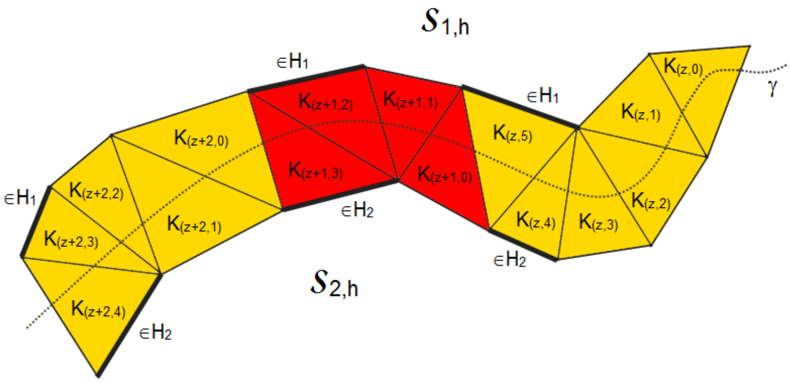

Figure 6: An example of the subdivision of $\mathcal{G}_h$ in groups.

$m_{(z,1),2,2} = 0$ That is:

$$\begin{aligned} s_{(z,0)} &= l^{-1}_{(z,0),3}\big(- c_{(z,0),3}\eta_i^{-1} p_{(z,0),i,h}|K_{(z,0)}| + c_{(z,0),3} l_{(z,0),1} m_{(z-1,N_{t,z-1}),1,2} \\ &\quad - c_{(z,0),1} l_{(z,0),3} m_{(z-1,N_{t,z-1}),1,2}\big), \\ s_{(z,1)} &= l^{-1}_{(z,1),2}\big(- c_{(z,1),2}\eta_i^{-1} p_{(z,1),i,h}|K_{(z,1)}| + c_{(z,1),2} l_{(z,1),1} m_{(z,0),2,2} \\ &\quad - c_{(z,1),1} l_{(z,1),2} m_{(z,0),2,2}\big), \end{aligned}$$

with the convention $m_{(z-1,N_{t,z-1}),1,2} = 0$ for $z = 0$. In this way, for every z and for $i = 1$ we obtain $m_{(z,0),1,2} = 0$ and

$$\begin{aligned} |m_{(z,0),1,3}| \le{}& |a_{(z,0),3}|\eta_1^{-1}|p_{(z,0),1,h}||K_{(z,0)}| + |b_{(z,0),3}||m_{(z-1,N_{t,z-1}),1,2}| \\ &+ |q_{(z,0),3}||s_{(z,0)}|. \end{aligned}$$

Since $m_{(z,0),1,2} = 0$, we have $|s_{(z,1)}| \le |c_{(z,1),2}|(l_{(z,1),2}\eta_1)^{-1}|p_{(z,1),1,h}||K_{(z,1)}|$ and then

$$\begin{aligned} |m_{(z,1),1,2}| &\le |a_{(z,1),2}|\eta_1^{-1}|p_{(z,1),1,h}||K_{(z,1)}| + |q_{(z,1),2}|\frac{|c_{(z,1),2}|}{l_{(z,1),2}}\eta_1^{-1}|p_{(z,1),1,h}||K_{(z,1)}| \\ &\le \frac{2C_\rho}{l_{(z,1),min}}\eta_1^{-1}|p_{(z,1),1,h}||K_{(z,1)}| \end{aligned}$$

and

$$\begin{aligned} |m_{(z,1),1,3}| &\le |a_{(z,1),3}|\eta_1^{-1}|p_{(z,1),1,h}||K_{(z,1)}| + |q_{(z,1),3}|\frac{|c_{(z,1),2}|}{l_{(z,1),2}}\eta_1^{-1}|p_{(z,1),1,h}||K_{(z,1)}|. \\ &\le \frac{2C_\rho}{l_{(z,1),min}}\eta_1^{-1}|p_{(z,1),1,h}||K_{(z,1)}| \end{aligned}$$

Now, we take $s_{(G_z,t)} = 0$ for every $1 < t < N_{G_z} - 2$, so that

$$\begin{aligned} |m_{(z,t),1,2}| &\le |a_{(z,t),2}|\eta_1^{-1}|p_{(z,t),1,h}||K_{(z,t)}| + |b_{(z,t),2}||m_{(z,t-1),1,2}| \\ &\le \frac{1}{l_{(z,t),min}}\eta_1^{-1}|p_{(z,t),1,h}||K_{(z,t)}| + C_\rho d_\phi|m_{(z,t-1),1,2}|. \end{aligned}$$

Iterating on t, we obtain:

$$|m_{(z,t),1,2}| \le 2C_\rho^t d_{\boldsymbol{\phi}}^{t-1}\eta_1^{-1}\sum_{k=1}^{t}\frac{|K_{(z,k)}|}{l_{(z,k),min}}|p_{(z,k),1,h}|,$$

for every $1 < t < N_{G_z}-2$ and hence

$$|m_{(z,t),1,2}| \le 2C_\rho^M d_{\boldsymbol{\phi}}^{M-1}\eta_1^{-1}\sum_{k=1}^{N_{G_z}}\frac{|K_{(z,k)}|}{l_{(z,k),min}}|p_{(z,k),1,h}|, \tag{22}$$

Analogously we can obtain the same estimate for $|m_{(z,t),1,3}|$. It is important to notice that inequality (22) is valid for $E_{(z,t),1,3} \notin H_1$. Then, for $t = N_{G_z}-2$ and $N_{G_z}-1$ we have that $E_{(z,N_{G_z}-2),3}$ and $E_{(z,N_{G_z}-1),3}$ belong to H_i for some i, and we will decide the value of $s^{(z,N_{G_z}-1)}$, $s^{(z,N_{G_z}-2)}$ later, to verify some conditions on $\mathcal{S}_{i,h}$. For now it is sufficient to know that we will choose them such that, for $r = 2,3$ and $k = 1,2$:

$$|m_{(z,N_{G_z}-k),1,r}| \le 2(M+1)C_\rho^{2M} d_{\boldsymbol{\phi}}^{M-1}\eta_1^{-1}\sum_{K\in SG_{1,z}}\frac{|K|}{l_{K,min}}|p_{K,1,h}|, \tag{23}$$

where $SG_{1,z}$ is a set containing all the elements of G_z and some elements of $\mathcal{S}_{1,h}$ such that $\mathrm{card}(SG_{1,z}) \le 3M$. We obtain

$$\begin{aligned}|m_{(z,0),1,3}| &\le |a_{(z,0),3}|\eta_1^{-1}|p_{(z,0),1,h}||K_{(z,0)}| + |b_{(z,0),3}||m_{(z-1,N_{t,z-1}),1,2}| \\ &+ |q_{(z,0),3}||s_{(z,0)}| \le 8(M+1)C_\rho^{2M+2} d_{\boldsymbol{\phi}}^{M}\eta_1^{-1}\sum_{K\in SG_{1,z}}\frac{|K|}{l_{K,min}}|p_{K,1,h}|\end{aligned}$$

where we exploited the fact that $|q_{(z,0),3}||c_{(z,0),3}l_{(z,0),1} - c_{(z,0),1}l_{(z,0),3}|l^{-1}_{(z,0),3} \le {C_\rho}^2 d_{\boldsymbol{\phi}}$ thanks to (12) and (15). Hence, for $0 \le t \le N_{G_z}-1$ and $r = 1,2,3$ we have:

$$|m_{(z,t),1,r}| \le 8(M+1)C_\rho^{2M+2} d_{\boldsymbol{\phi}}^{M}\eta_1^{-1}\sum_{K\in SG_{1,z}}\frac{|K|}{l_{K,min}}|p_{K,1,h}|.$$

Using analogous arguments we can prove the same for $|m_{(z,t),2,r}|$, and setting $C = 8(M+1)C_\rho^{2M+2} d_{\boldsymbol{\phi}}^{M}$, for every $0 \le t \le N_{G_z}-1$, $i = 1,2$, $r = 1,2,3$, we obtain:

$$|m_{(z,t),i,r}| \le C\eta_i^{-1}\sum_{K\in SG_{i,z}}\frac{|K|}{l_{K,min}}|p_{K,i,h}|.$$

It is important to notice that C does not depend on h. If we had not use the subdivision of $\mathcal{G}_h$ into groups, *i.e.* considering $\mathcal{G}_h$ as a single group, we would have obtained a constant C not depending on M but on N_{G_z}, which clearly grows when $h \to 0$, and thus our constant C would increase indefinitely when $h \to 0$. The subdivision in the subgroups has allowed us to keep C independent from h.
We are now in the position to write that for every j

$$\begin{aligned}&\|\eta_i^{\frac{1}{2}}\widetilde{\boldsymbol{v}}_{K_{j,i},h}\|_{H^1(K_{j,i})} \lesssim \sum_{r=1}^{3}\eta_i^{\frac{1}{2}}|m_{j,i,r}|\|\boldsymbol{\phi}_{j,i,r}\|_{H^1(K_{j,i})} \\ &\lesssim \eta_i^{\frac{1}{2}}\left(C\eta_i^{-1}\sum_{K\in SG_{i,z}}\frac{|K|}{l_{K,min}}|p_{K,i,h}|\right)\left(\sum_{r=1}^{3}\|\boldsymbol{\phi}_r\|_{H^1(K_{j,i})}\right).\end{aligned} \tag{24}$$

Thanks to inverse inequalities, we have $\|\boldsymbol{\phi}_r\|_{H^1(K_{j,i})} \lesssim h^{-1}|K_{j,i}|^{\frac{1}{2}}$ and, thanks to shape regularity, $|K|l_{K,min}^{-1} \lesssim h$ for every k. Hence,

$$\|\eta_i^{\frac{1}{2}}\widetilde{\boldsymbol{v}}_{K_{j,i},h}\|_{H^1(K_{j,i})} \lesssim C\eta_i^{-\frac{1}{2}}|K_{j,i}|^{\frac{1}{2}} \sum_{K\in SG_{i,z}} |p_{K,i,h}|$$

and finally by, setting $\widetilde{\boldsymbol{v}}_{\mathcal{G}_h} = \sum_{K\in\mathcal{G}_h} \widetilde{\boldsymbol{v}}_{K_{j,i},h}$, we have

$$\begin{aligned}\|\eta_i^{\frac{1}{2}}\widetilde{\boldsymbol{v}}_{\mathcal{G}_h}\|_{H^1(\mathcal{G}_h)} &\lesssim \sum_{j=0}^{N_{\mathcal{G}_h}-1} \|\eta_i^{\frac{1}{2}}\widetilde{\boldsymbol{v}}_{K_{j,i},h}\|_{H^1(K_{j,i})} \lesssim C\eta_i^{-\frac{1}{2}} \sum_{j=0}^{N_{\mathcal{G}_h}-1} |K_{j,i}|^{\frac{1}{2}} \sum_{K\in\mathcal{G}_h,\mathcal{S}_{i,h}} |p_{K,i,h}| \\ &\lesssim C\eta_i^{-\frac{1}{2}} \sum_{K\in\mathcal{G}_h,\mathcal{S}_{i,h}} |K|^{\frac{1}{2}}|p_{K,i,h}| \lesssim C\|\eta^{-\frac{1}{2}}p_h\|_{L^2(\mathcal{G}_h\cup\mathcal{S}_{i,h})} \lesssim C\|\eta^{-\frac{1}{2}}p_h\|_{L^2(\mathcal{SGS}_h)}.\end{aligned} \tag{25}$$

Part 3b - Subdomains $\mathcal{S}_{1,h}$, $\mathcal{S}_{2,h}$. Now we consider $\mathcal{S}_{i,h}$. We indicate with $N_{\mathcal{S}_{i,h}}$ the number of elements of $\mathcal{S}_{i,h}$, and we enumerate them from 0 to $N_{\mathcal{S}_{i,h}} - 1$ in this way: we choose $Q_{0,i}$ such that it has an edge in common with $\partial\Omega$, and a vertex in common with $K_0 \in \mathcal{G}_h$, then we choose every $Q_{j,i}$ such that it has an edge in common with $Q_{j-1,i}$. Given an element $Q_{j,i} \in \mathcal{S}_{i,h}$, we build $\widetilde{\boldsymbol{v}}_{Q_{j,i},h} \in \mathbb{RT}_0(Q_{j,i})$ such that

$$b(p_h, \hat{p}_h, \widetilde{\boldsymbol{v}}_{Q_{j,i},h}, \mathbf{0}) \gtrsim \|\eta^{-\frac{1}{2}}p_h\|^2_{L^2(Q_{j,i})}$$

As we did for $\mathcal{G}_h$, if we find a $\widetilde{\boldsymbol{v}}_{Q_{j,i},h} \in \mathbb{RT}_0(Q_{j,i})$ such that $-\nabla\cdot\widetilde{\boldsymbol{v}}_{Q_{j,i},h} \gtrsim \eta_i^{-1}p_{j,i,h}$ on $Q_{j,i}$, with $p_{j,i,h} = p_h|_{Q_{j,i}}$, we have

$$b(p_h, \hat{p}_h, \widetilde{\boldsymbol{v}}_{Q_{j,i},h}, \mathbf{0}) = -\left(p_h, \nabla\cdot\widetilde{\boldsymbol{v}}_{Q_{j,i},h}\right)_{Q_{j,i}} \gtrsim \|\eta^{-1}p_h\|^2_{L^2(Q_{j,i})} \tag{26}$$

and the first inequality of the inf-sup condition is satisfied. To this purpose we enumerate the edges of the element $Q_{j,i} \in \mathcal{S}_{i,h}$, calling them $E_{j,i,r}$ for $r = 1, 2, 3$. We observe that every element $Q_{j,i} \in \mathcal{S}_{i,h}$ has one and only one edge that is either in common with $\partial\mathcal{G}_h$ or in common with $\partial\mathcal{T}_{i,h}$, and we call it $E_{j,i,3}$. For $Q_{0,i}$ we call $E_{0,i,1}$ the edge in common with $\partial\Omega$, and obviously $E_{0,i,2}$ the other one. Then, we enumerate the edges $E_{j,i,1}$, $E_{j,i,2}$ for $j \geq 1$ so that $E_{j,i,1} = E_{j-1,i,2}$. Finally, we call $m_{j,i,r}$ the *d.o.f.* corresponding to edge $E_{j,i,r}$. Writing $\widetilde{\boldsymbol{v}}_{Q_{j,i},h} = m_{j,i,1}\boldsymbol{\phi}_{j,1} + m_{j,i,2}\boldsymbol{\phi}_{j,2} + m_{j,i,3}\boldsymbol{\phi}_{j,3}$ and proceeding as for $\mathcal{G}_h$ we obtain that $-\nabla\cdot\widetilde{\boldsymbol{v}}_{Q_{j,i},h} = \eta_i^{-1}p_{j,i,h}$ is equivalent to

$$-m_{j,i,1}l_{j,i,1} - m_{j,i,2}l_{j,i,2} - l_{j,i,3}m_{j,i,3} = \eta_i^{-1}p_{j,i,h}|Q_{j,i}|.$$

If $E_{0,i,3}$ is in common with $\partial\mathcal{G}_h$, $m_{0,i,3}$ is determined by the value of the *d.o.f.* on the same edge. On the contrary, if $E_{0,i,3}$ is in common with $\partial\mathcal{T}_{i,h}$ we must set $m_{0,i,3} = 0$. To verify the desired the first condition in (20), we set $m_{0,i,1} = 0$ and

$$m_{0,i,2} = a_{0,i}\eta_i^{-1}p_{0,i,h}|Q_{0,i}| + b_{0,i}m_{0,i,3},$$

where $a_{0,i} = -l_{0,i,2}^{-1}$, $b_{0,i} = -l_{0,i,3}l_{0,i,2}^{-1}$. For $j \geq 1$, since $E_{j,i,1} = E_{j-1,i,2}$, for continuity we must have $m_{j,i,1} = -m_{j-1,i,2}$, and so we need to take

$$m_{j,i,2} = a_{j,i}\eta_i^{-1}p_{j,i,h}|Q_{j,i}| + b_{j,i}m_{j,i,3} + c_{j,i}m_{j-1,i,2},$$

where $a_{j,i} = -l_{j,i,2}^{-1}$, $b_{j,i} = -l_{j,i,3}l_{j,i,2}^{-1}$, $q_{j,i} = l_{j,i,1}l_{j,i,2}^{-1}$. Hence for every $Q_{j,i}$ we have built a function $\widetilde{\boldsymbol{v}}_{Q_{j,i},h} = m_{j,i,1}\boldsymbol{\phi}_{j,1} + m_{j,i,2}\boldsymbol{\phi}_{j,2} + m_{j,i,3}\boldsymbol{\phi}_{j,3}$, that satisfies the first inequality. It remains to show that $\widetilde{\boldsymbol{v}}_{Q_{j,i},h}$ satisfies also the second inequality in (20) for every Q_j, that is $\|\eta_i^{\frac{1}{2}}\widetilde{\boldsymbol{v}}_h\|_{H^1(\mathcal{S}_{i,h})} \lesssim \|\eta^{-\frac{1}{2}}p_h\|_{L^2(\Omega)}$ for $i = 1, 2$. For every j, we have $|a_{j,i}| = |-l_{j,i,2}^{-1}| \leq l_{j,i,min}^{-1}$, $|b_{j,i}| = |-l_{j,i,3}l_{j,i,2}^{-1}| \leq C_\rho$, $|c_{j,i}| = |l_{j,i,1}l_{j,i,2}^{-1}| \leq C_\rho$.

Now, we divide the elements of $\mathcal{S}_{i,h}$ into groups. Starting from $Q_{0,i}$ every group $S_{i,z}$ for $z = 1, \ldots, N_{S_{i,z}}$ is made by a first element that has one edge belonging to H_i and by all the successive elements up to the next element that has an element belonging to H_i (this element will be the first element of the successive group). If $Q_{0,i}$ does not have an element belonging to H_i, then we consider as first group $S_{i,0}$ the set of elements up to the first that has one edge belonging to H_i, and in order not to consider this group in a special way we introduce for this group a "virtual" first element Q^* that has $m_{Q^*i,1} = m_{Q^*,i,2} = m_{Q^*,i,3} = 0$, so that all the inequalities that we will show for all the other groups are true also for this first group. We indicate with (z, t) the index, in the global enumeration Q_j, of the t^{th} element of the z^{th} group, thus $Q_{(z,t),i}$ are the elements of $S_{i,z}$ for $t = 0, \ldots, N_{S_{i,z}} - 1$. We recall that in $\hat{\gamma}_{G,i,h}$ between edges of H_i there can be at most M_0 edges not belonging to H_i. Then every $S_{i,z}$ has at most M_0 elements of $\mathcal{S}_{i,h}$ that have an edge in common with $\mathcal{G}_h$, and between two elements with an edge in common with $\mathcal{G}_h$ there are at most $N_{S,h} (\leq M_0)$ elements that have one edge in common with $\mathcal{T}_{i,h}$. Consequently by construction we have $N_{S_{i,z}} \leq M_0(M_0 + 1) = M$. See Figure 7 for an example. By construction element $Q_{(z,0),i}$ is such that $E_{(z,0),i,3} \in H_i$ and hence

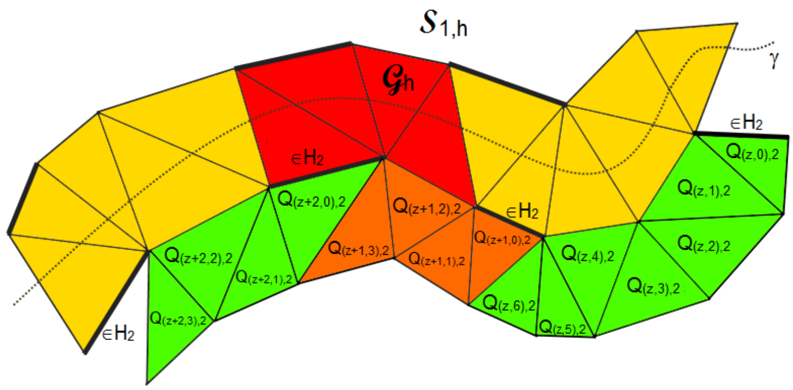

Figure 7: An example of the subdivision of $\mathcal{S}_{2,h}$ in groups

we can choose the value of $m_{(z,0),1,3}$. We take it such that $m_{(z,0),1,2} = 0$, that is

$$m_{(z,0),1,3} = \big(-a_{(z,0),1}\eta_1^{-1}p_{(z,0),1,h}|Q_{(z,0),1}| - c_{(z,0),1}m_{(z-1,N_{S_{z-1}}-1),1,2}\big)b_{(z,0),1}^{-1}.$$

By construction, for every element $Q_{(z,t),1}$ of $S_{1,z}$, for $t = \{1, 2, ...\}$ we have that $E_{(z,t),1,3}$ is either in common with $\mathcal{G}_h$ (with $E_{(z,t),1,3} \notin H_1$), or with $\mathcal{T}_{1,h}$. In the former case, recalling (22), we have

$$|m_{(z,t),1,3}| \leq 2C_\rho^M d_{\boldsymbol{\phi}}^{M-1}\eta_1^{-1} \sum_{K \in G_{1,z,t}} \frac{|K|}{l_{K,min}}|p_{K,1,h}|,$$

where $G_{1,z,t}$ is the group of elements in $\mathcal{G}_h$ element having an edge in common with $Q_{(z,t),1}$. In the latter, case we have $|m_{(z,t),1,3}| = 0$. We observe that for each $Q_{(z,t),1}$ we have at most two distinct $G_{1,z,t}$, and we call $G_{1,z}$ the union of these two groups, thus $\text{card}(G_{1,z}) \leq 2M$. Hence, for $t = 1$ we obtain

$$|m_{(z,1),1,2}| \leq \frac{|Q_{(z,1),1}|}{l_{(z,1),1,min}} \eta_1^{-1} |p_{(z,1),1,h}| + 2C_\rho^M d_{\boldsymbol{\phi}}^{M-1} \eta_1^{-1} \sum_{K \in G_{1,z,1}} \frac{|K|}{l_{K,min}} |p_{K,1,h}|,$$

and for $t = 2$

$$\begin{aligned}
|m_{(z,2),1,2}| &\leq \frac{|Q_{(z,2),1}|}{l_{(z,2),1,min}} \eta_1^{-1} |p_{(z,2),1,h}| + C_\rho \frac{|Q_{(z,1),1}|}{l_{(z,1),1,min}} \eta_1^{-1} |p_{(z,1),1,h} \\
&+ 4C_\rho^{M+1} d_{\boldsymbol{\phi}}^{M-1} \eta_1^{-1} \sum_{K \in G_{1,z,2}} \frac{|K|}{l_{K,min}} |p_{K,1,h}| \\
&\leq C_\rho \eta_1^{-1} \left(\frac{|Q_{(z,2),1}|}{l_{(z,2),1,min}} \eta_1^{-1} |p_{(z,2),1,h}| + \frac{|Q_{(z,1),1}|}{l_{(z,1),1,min}} \eta_1^{-1} |p_{(z,1),1,h}| \right) \\
&+ 4C_\rho^{M+1} d_{\boldsymbol{\phi}}^{M-1} \eta_1^{-1} \sum_{K \in G_{1,z}} \frac{|K|}{l_{K,min}} |p_{K,1,h}|,
\end{aligned}$$

where we used the fact that $C_\rho \geq 1$. For $t > 2$ we obtain:

$$\begin{aligned}
|m_{(z,t),1,2}| \leq C_\rho^{t-1} \eta_1^{-1} \sum_{k=1}^{t} \frac{|Q_{(z,k),1}|}{l_{(z,k),1,min}} \eta_1^{-1} |p_{(z,k),1,h}| \\
+ 2tC_\rho^{M+t-1} d_{\boldsymbol{\phi}}^{M-1} \eta_1^{-1} \sum_{K \in G_{1,z}} \frac{|K|}{l_{K,min}} |p_{K,1,h}|.
\end{aligned}$$

Hence we have, for every j:

$$|m_{(z,t),1,2}| \leq 2MC_\rho^{2M-1} d_{\boldsymbol{\phi}}^{M-1} \eta_1^{-1} \sum_{Q \in (S_{1,z} \setminus \{Q_{(z,0),1}\}) \cup G_{1,z}} \frac{|Q|}{l_{Q,min}} |p_{Q,1,h}|. \tag{27}$$

Thanks to (27) we can write:

$$\begin{aligned}
|m_{(z,0),1,3}| &\leq C_\rho \eta_1^{-1} |p_{(z,0),1,h}| |Q_{(z,0),1}| + C_\rho |m_{(z-1,N_{S_{z-1}}-1),1,2}| \\
&\leq 2(M+1) C_\rho^{2M} d_{\boldsymbol{\phi}}^{M-1} \eta_1^{-1} \sum_{Q \in S_{1,z} \cup G_{1,z}} \frac{|Q|}{l_{Q,min}} |p_{Q,1,h}|,
\end{aligned}$$

with $\text{card}(Q_{(z,1),1} \cup G_{1,z}) \leq 3M$: this is exactly what we supposed for $m_{Q,1,3} = m_{(z,N_{G_z}-k),1,r}$ in (23) for any Q that has an edge in H_1. More generally, we obtain that for every t, r, z:

$$|m_{(z,t),1,r}| \leq 2(M+1) C_\rho^{2M} d_{\boldsymbol{\phi}}^{M-1} \eta_1^{-1} \sum_{Q \in S_{1,z} \cup G_{1,z}} \frac{|Q|}{l_{Q,min}} |p_{Q,1,h}|.$$

Using analogous arguments we can prove the same for $|m_{(z,t),2,r}|$. For simplicity we set $C = 2(M+1) C_\rho^{2M} d_{\boldsymbol{\phi}}^{M-1}$ and we set $SG_{i,z} = S_{i,z} \cup G_{i,z}$, so that

$$|m_{j,i,r}| \leq C \eta_i^{-1} \sum_{Q \in SG_{i,z}} \frac{|Q|}{l_{Q,min}} |p_{Q,i,h}|.$$

With the same arguments used in (24), (25), we obtain

$$\|\eta_i^{\frac{1}{2}} \widetilde{\boldsymbol{v}}_{\mathcal{S}_{i,h}}\|_{H^1(\mathcal{S}_{i,h})} \lesssim C\|\eta^{-\frac{1}{2}} p_h\|_{L^2(\mathcal{SGS}_h)}. \tag{28}$$

To conclude, we set $\widetilde{\boldsymbol{v}}_h = \widetilde{\boldsymbol{v}}_{\mathcal{G}_h} + \widetilde{\boldsymbol{v}}_{\mathcal{S}_{1,h}} + \widetilde{\boldsymbol{v}}_{\mathcal{S}_{2,h}}$, and we have that

$$b(p_h, \widetilde{\boldsymbol{v}}_h) \gtrsim \|\eta^{-\frac{1}{2}} p_h\|^2_{L^2(\mathcal{SGS}_h)} \quad \|\eta_i^{\frac{1}{2}} \widetilde{\boldsymbol{v}}_h\|_{H^1(\mathcal{SGS}_h)} \lesssim \|\eta_i^{-\frac{1}{2}} p_{i,h}\|_{L^2(\mathcal{SGS}_h)}.$$

where we used (21), (25), (26), (28). Therefore (19) is satisfied ad this concludes the proof. □

4.4 Stability

The inf-sup condition implies a stability result.

Theorem 1 (Stability) *Let $(\boldsymbol{u}_h, \hat{\boldsymbol{u}}_h, p_h, \hat{p}_h) \in \mathbf{W}_h$, and let $M_{\hat{\gamma}}$ be the constant of Theorem 4.1. Then,*

$$\|(\boldsymbol{u}_h, \hat{\boldsymbol{u}}_h, p_h, \hat{p}_h)\|_{\mathbf{W}_h} \lesssim M_{\hat{\gamma}} \sup_{\mathbf{W}_h} \frac{\mathcal{C}((\boldsymbol{u}_h, \hat{\boldsymbol{u}}_h, p_h, \hat{p}_h), (\boldsymbol{v}_h, \hat{\boldsymbol{v}}_h, q_h, \hat{q}_h))}{\|(\boldsymbol{v}_h, \hat{\boldsymbol{v}}_h, q_h, \hat{q}_h)\|_{\mathbf{W}_h}}. \tag{29}$$

Proof. The proof is analogous to the proof of stability in [7]. In particular, in the proof we used congruence (7), boundedness (10), inf-sup condition (16). □

4.5 Convergence

Thanks to the previous stability result, we can state the convergence of our numerical scheme in a standard way.

Theorem 2 (Convergence) *Let $(\boldsymbol{u}, \hat{\boldsymbol{u}}, p, \hat{p}) \in \mathbf{W}$ be the solution of problem (2). There exists a unique solution $(\boldsymbol{u}_h, \hat{\boldsymbol{u}}_h, p_h, \hat{p}_h) \in \mathbf{W}_h$ of problem (6), and*

$$\|(\boldsymbol{u}_h - \boldsymbol{u}, \hat{\boldsymbol{u}}_h - \hat{\boldsymbol{u}}, p_h - p, \hat{p}_h - \hat{p})\|_{\mathbf{W}_h} \lesssim M_{\hat{\gamma}} \inf_{\mathbf{W}_h} \|(\boldsymbol{v}_h - \boldsymbol{u}, \hat{\boldsymbol{v}}_h - \hat{\boldsymbol{u}}, q_h - p, \hat{q}_h - \hat{p})\|_{\mathbf{W}_h}.$$

Proof. The proof is analogous to the proof of convergence in [7]. In particular, in the proof boundedness (10), positivity (11) and stability (29) are used. □

We notice that, since $M_{\hat{\gamma}}$ is not dependent on h, the estimate is asymptotically robust as $h \to 0$.

5 Numerical examples

In this section we assess the theoretical results proven in Section 4 considering a test case where the fracture exhibits a sharp bend in a relatively coarse grid. Then, we validate the numerical method studying the error and the related order of convergence.

5.1 Stability analyses

Let us consider a domain $\Omega = (0,1)^2$ cut by a fracture $\hat{\gamma}$ described by the following equation

$$\hat{\gamma} = \left\{ (x,y) \in \mathbb{R}^2 : \, y = \begin{cases} mx + \dfrac{m-1}{2} & \text{if } x < \dfrac{1}{2} \\ -mx + \dfrac{m+1}{2} & \text{if } x \geq \dfrac{1}{2} \end{cases} \right\}.$$

with the same permeability as the bulk medium (set to 1 for simplicity) and aperture $l_{\hat{\gamma}} = 0.01$. We consider two different slopes, $m = m_1 = 1.3$ and $m = m_2 = 1.5$, corresponding to the angles $\theta_1 = 75.13°$ and $\theta_2 = 67.38°$ at the corner ($x = 0.5$) respectively. In both cases we consider a coarse bulk grid with $h \simeq 0.08$ that satisfies Assumptions H1 and H2. We impose homogeneous Neumann boundary conditions and a constant source term $f = 4$. Despite the small difference between the two configurations the solutions, shown in Figure 8, are completely different. In the first case we obtain the correct solution, while in the second we can observe oscillations in some cut elements close to the angle vertex (more visible in the zoom in Figure 10). Indeed, in this second configuration the inf-sup condition is not satisfied. Let us consider the two cut regions shown in Figure 9: with $m_2 = 1.5$ and the given grid we have some non-cut edges that are shared by two triangles of the cut region, and this violates Hypothesis 3.

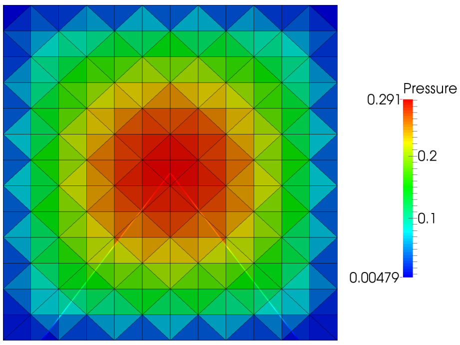

(a) Solution for m_1

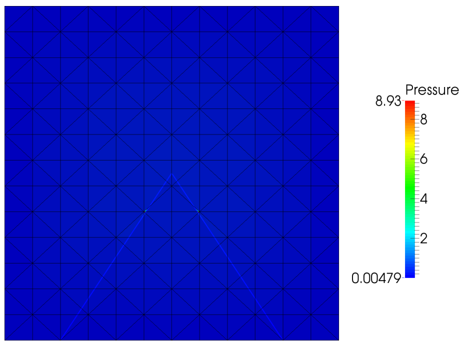

(b) Solution for m_2

Figure 8: Pressure in the bulk and the fracture in the case with slope m_1 and m_2.

5.2 Convergence

To test the converge of the method we consider the test case reported in [16]. For this purpose we consider a domain $\Omega = (-1,1)^2$ and we take $\boldsymbol{\Lambda}_j = \boldsymbol{I}$ for the porous media Ω_1 and Ω_2. The domain is cut by an horizontal fracture $\hat{\gamma}$ of

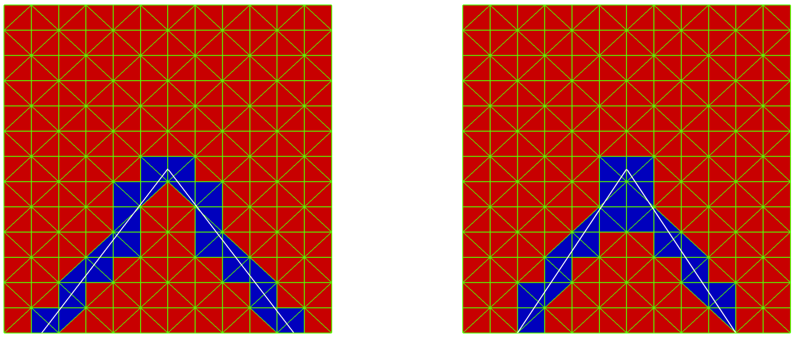

(a) Cut region for m_1 (b) Cut region for m_2

Figure 9: Cut region and fracture configuration for m_1 and m_2.

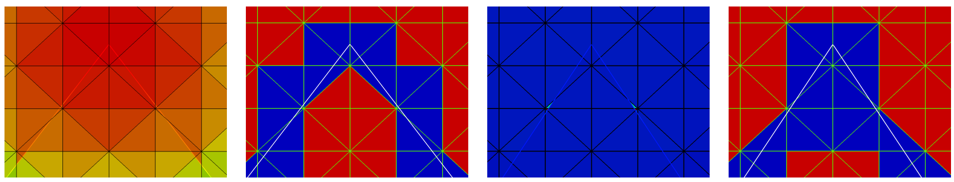

(a) Solution for m_1 (b) Cut region for m_1 (c) Solution for m_2 (d) Cut region for m_2

Figure 10: Zoom of the solutions and corresponding cut regions for m_1 and m_2.

thickness $l_{\hat{\gamma}}$ in $x = 0$. The fracture is isotropic, and so the permeability tensor is $\boldsymbol{\Lambda}_f = \lambda_f \boldsymbol{I}$ with $\lambda_f \in \mathbb{R}^+$. The problem is the one described by equations (2) and the exact solution we have considered is

$$p_{ex}(x,y) = \begin{cases} \lambda_f \cos(x)\cosh(y) + (1-\lambda_f)\cosh\left(\frac{l_{\hat{\gamma}}}{2}\right)\cos(x) & \text{on } \Omega \setminus \hat{\gamma} \\ \cos(x)\cosh(y) & \text{on } \hat{\gamma} \end{cases},$$

obtained by imposing $\boldsymbol{f} = 0$ and $f(x,y) = (1-\lambda_f)\cosh\left(\frac{l_{\hat{\gamma}}}{2}\right)\cos(x)$ on $\Omega \setminus \hat{\gamma}$, 0 otherwise. We assume homogeneous Neumann boundary conditions both on $\partial\Omega \setminus \partial\hat{\gamma}$ and on $\partial\hat{\gamma}$. In the simulations we use a constant thickness of the fracture equal to $l_{\hat{\gamma}} = 10^{-3}$, and we change the fracture permeability: $\lambda_f = 10^{-3}$, $\lambda_f = 1$ and $\lambda_f = 10^3$. For every different λ_f we consider five different values of h. The errors are calculated for the pressure p in the domain $\Omega \setminus \hat{\gamma}$ as:

$$err = \frac{|||p_{ex} - p_h|||}{|||p_{ex}|||} = \sqrt{\frac{\sum_{K \in \mathcal{T}_h} \frac{1}{|K|} \int_K (p_{ex} - p_h)^2}{\sum_{K \in \mathcal{T}_h} \frac{1}{|K|} \int_K p_{ex}^2}}$$

In Figure 11 the variation of err as function of h with constant λ_f is shown, and we observe that the order of convergence of the pressure is approximately linear.

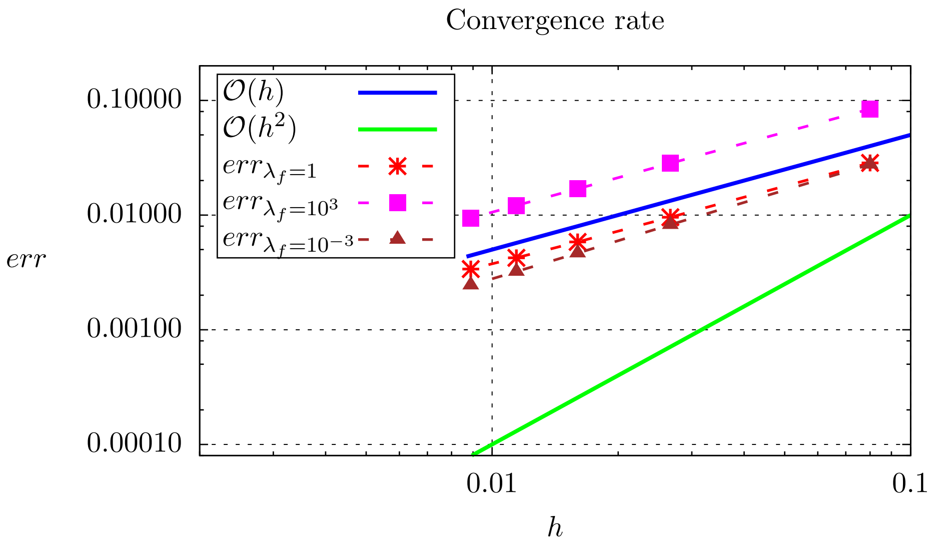

Figure 11: Computed errors in function of h for different values of λ_f.

6 Conclusion

In this work we considered a suitable XFEM-type enrichment for the mixed finite element approximation of a Darcy problem in fractured porous media. The fracture is considered as an object of co-dimension one, see [2, 20, 3], and its geometrical representation is irrespective of the grid of the porous medium, see [17, 7]. The well posedness proof in [7] considers the case of known pressure and Darcy velocity in the fracture, however the authors showed numerical evidences that it is indeed satisfied in the general case. For this reason we focused this paper on the well posedness of the discrete coupled problem, *i.e.* where pressure and Darcy velocity are both considered as unknowns in the fracture and in the porous media. This result requires more advanced techniques than in [7]. The numerical results confirm that the hypotheses on the grid and fracture configuration for the inf-sup condition, presented in Subsection 4.3, are rather sharp. However we remark that given a fracture geometry it is easy to find a mesh with suitable grid size that fulfils the necessary hypotheses. Finally we assessed the order of convergence against an exact solution.

7 Acknowledgements

The authors wish to thank Lourenço Beirão da Veiga, Antonio Cervone, Luca Formaggia and Guido Iori for many fruitful discussions.

References

[1] Omar Al-Hinai, Sanjay Srinivasan, Mary F Weeler, et al. Mimetic finite differences for flow in fractures from microseismic data. In *SPE Reservoir Simulation Symposium.* Society of Petroleum Engineers, 2015.

[2] Clarisse Alboin, Jérôme Jaffré, Jean E. Roberts, Xuewen Wang, and Christophe Serres. *Domain decomposition for some transmission problems in flow in porous media*, volume 552 of *Lecture Notes in Phys.*, pages 22–34. Springer, Berlin, 2000.

[3] Philippe Angot, Franck Boyer, and Florence Hubert. Asymptotic and numerical modelling of flows in fractured porous media. *M2AN Math. Model. Numer. Anal.*, 43(2):239–275, 2009.

[4] Paola F. Antonietti, Luca Formaggia, Anna Scotti, Marco Verani, and Nicola Verzotti. Mimetic finite difference approximation of flows infractured porous media. Technical report, Politecnico di Milano, 2015.

[5] Matías Fernando Benedetto, Stefano Berrone, Sandra Pieraccini, and Stefano Scialò. The virtual element method for discrete fracture network simulations. *Computer Methods in Applied Mechanics and Engineering*, 280(0):135–156, 2014.

[6] Franco Brezzi and Michel Fortin. *Mixed and Hybrid Finite Element Methods*, volume 15 of *Computational Mathematics.* Springer Verlag, Berlin, 1991.

[7] Carlo D'Angelo and Anna Scotti. A mixed finite element method for Darcy flow in fractured porous media with non-matching grids. *Mathematical Modelling and Numerical Analysis*, 46(02):465–489, 2012.

[8] Jim Douglas and Todd Arbogast. Dual porosity models for flow in naturally fractured reservoirs. In John H. Cushman, editor, *Dynamics of Fluids in Hierarchical Porous Media*, pages 177–221, London, 1990. Academic Press.

[9] Alexandre Ern and Jean-Luc Guermond. *Theory and practice of finite elements.* Applied mathematical sciences. Springer, 2004.

[10] Isabelle Faille, Eric Flauraud, Frédéric Nataf, Sylvie Pégaz-Fiornet, Frédéric Schneider, and Françoise Willien. A new fault model in geological basin modelling. Application of finite volume scheme and domain decomposition methods. In *Finite volumes for complex applications, III (Porquerolles, 2002)*, pages 529–536. Hermes Sci. Publ., Paris, 2002.

[11] Luca Formaggia, Alessio Fumagalli, Anna Scotti, and Paolo Ruffo. A reduced model for Darcy's problem in networks of fractures. *ESAIM: Mathematical Modelling and Numerical Analysis*, 48:1089–1116, 7 2014.

[12] Alessio Fumagalli and Anna Scotti. A numerical method for two-phase flow in fractured porous media with non-matching grids. *Advances in Water Resources*, 62, Part C(0):454–464, 2013. Computational Methods in Geologic CO2 Sequestration.

[13] Alessio Fumagalli and Anna Scotti. A reduced model for flow and transport in fractured porous media with non-matching grids. In Andrea Cangiani, Ruslan L. Davidchack, Emmanuil Georgoulis, Alexander N. Gorban, Jeremy Levesley, and Michael V. Tretyakov, editors, *Numerical Mathematics and Advanced Applications 2011*, pages 499–507. Springer Berlin Heidelberg, 2013.

[14] Alessio Fumagalli and Anna Scotti. An efficient xfem approximation of darcy flow in arbitrarly fractured porous media. *Oil and Gas Sciences and Technologies - Revue d'IFP Energies Nouvelles*, 69(4):555–564, April 2014.

[15] Vivette Girault and Pierre-Arnaud Raviart. *Finite element methods and Navier-Stokes equations*, volume 5 of *Springer Series in Computational Mathematics*. Springer-Verlag Berlin Heidelberg, 1986.

[16] Håkon Hægland, Anongnart Assteerawatt, Helge K. Dahle, Geir Terje Eigestad, and Rainer Helmig. Comparison of cell- and vertex-centered discretization methods for flow in a two-dimensional discrete-fracture-matrix system. *Advances in Water Resources*, 32(12):1740–1755, 2009.

[17] Anita Hansbo and Peter Hansbo. An unfitted finite element method, based on Nitsche's method, for elliptic interface problems. *Comput. Methods Appl. Mech. Engrg.*, 191(47-48):5537–5552, 2002.

[18] Jérôme Jaffré, M. Mnejja, and Jean E. Roberts. A discrete fracture model for two-phase flow with matrix-fracture interaction. *Procedia Computer Science*, 4:967–973, 2011.

[19] Bradley T. Mallison, Mun-Hong Hui, and Wayne Narr. Practical Gridding Algorithms for Discrete Fracture Modeling Workflows. In *Ecmor XII*, number September 2010, 2010.

[20] Vincent Martin, Jérôme Jaffré, and Jean E. Roberts. Modeling fractures and barriers as interfaces for flow in porous media. *SIAM J. Sci. Comput.*, 26(5):1667–1691, 2005.

[21] Alfio Quarteroni and Alberto Valli. *Numerical approximation of partial differential equations*, volume 23 of *Springer Series in Computational Mathematics*. Springer-Verlag, Berlin, 1994.

[22] Jean E. Roberts and Jean-Marie Thomas. Mixed and hybrid methods. In *Handbook of numerical analysis, Vol. II*, Handb. Numer. Anal., II, pages 523–639. North-Holland, Amsterdam, 1991.